between 8:00 AM and 8:00 PM both in fed and 4-day fasted rats, although the expressions of renal PEPT1 and PEPT2 were increased in 4-day fasted rats. Although we did not assess the renal handling of CETB in detail, it is plausible that renal PEPT1 and PEPT2 may little affect the CETB pharmacokinetics.

CETB pharmacokinetic parameters such as C_{max} and $AUC_{0-3\ h}$ obtained by the intestinal administration were significantly larger in 4-day fasted rats compared with the fed rats. In addition, the CETB absorption rates assessed by the in situ loop technique in 4-day fasted rats were significantly increased compared with the fed rats both at 8:00 AM and at 8:00 PM. All these findings seemed to be accountable by increased intestinal PEPT1 protein expression. Recently, Naruhashi et al. (2002) reported that PEPT1 mRNA expression was induced by starvation and its level correlated with absorptive transport of cefadroxil, an oral β-lactam antibiotic, in the rat intestine. Furthermore, it was reported that the expression level of PEPT1 assessed by Western blot analysis in the rat jejunum was significantly correlated with intestinal loop single perfusion of another oral β-lactam antibiotic, cephalexin (Berlioz et al., 1999). All these findings suggested that the expression level of intestinal PEPT1 is one of the key factors determining the absorption of oral β-lactam antibiotics.

In conclusion, we have demonstrated that the diurnal rhythm of intestinal PEPT1 transport activity is altered by fasting. The diurnal rhythm of intestinal PEPT1 would be responsible for the diurnal variation for pharmacokinetics of peptide-like drugs such as CETB, which was also abolished by fasting.

References

Ahrén B (2000) Diurnal variation in circulating leptin is dependent on gender, food intake and circulating insulin in mice. *Acta Physiol Scand* **169:**325–331.

Ashida K, Katsura T, Motohashi H, Saito H, and Inui K (2002) Thyroid hormone regulates the activity and expression of the peptide transporter PEPT1 in Caco-2 cells. *Am J Physiol* **282:**G617–G623.

Berlioz F, Julien S, Tsocas A, Chariot J, Carbon C, Farinotti R, and Rozé C (1999) Neural modulation of cephalexin intestinal absorption through the di- and tripeptide brush border transporter of rat jejunum in vivo. *J Pharmacol Exp Ther* **288:**1037–1044.

Berlioz F, Maoret JJ, Paris H, Laburthe M, Farinotti R, and Rozé C (2000) α_2-Adrenergic receptors stimulate oligopeptide transport in a human intestinal cell line. *J Pharmacol Exp Ther* **294:**466–472.

Buyse M, Berlioz F, Guilmeau S, Tsocas A, Voisin T, Péranzi G, Merlin D, Laburthe M, Lewin MJ, Rozé C, et al. (2001) PepT1-mediated epithelial transport of dipeptides and cephalexin is enhanced by luminal leptin in the small intestine. *J Clin Investig* **108:**1483–1494.

Daniel H and Herget M (1997) Cellular and molecular mechanisms of renal peptide transport. *Am J Physiol* **273:**F1–F8.

Fisher RB and Gardner MLA (1976) Diurnal rhythm in the absorption of glucose and water by isolated rat small intestine. *J Physiol (Lond)* **254:**821–825.

Fujita T, Majikawa Y, Umehisa S, Okada N, Yamamoto A, Ganapathy V, and Leibach FH (1999) ς-Receptor ligand-induced up-regulation of the H^+/peptide transporter PEPT1 in the human intestinal cell line Caco-2. *Biochem Biophys Res Commun* **261:**242–246.

Gangopadhyay A, Thamotharan M, and Adibi SA (2002) Regulation of oligopeptide transporter (Pept-1) in experimental diabetes. *Am J Physiol* **283:**G133–G138.

Goo RH, Moore JG, Greenberg E, and Alazraki NP (1987) Circadian variation in gastric emptying of meals in humans. *Gastroenterology* **93:**515–518.

Inui K, Okano T, Takano M, Saito H, and Hori R (1984) Carrier-mediated transport of cephalexin via the dipeptide transport system in rat renal brush-border membrane vesicles. *Biochim Biophys Acta* **769:**449–454.

Inui K and Terada T (1999) Dipeptide transporters, in *Membrane Transporters as Drug Targets* (Amidon GL and Sadée eds) pp 269–288, Plenum Publishing Corporation, New York.

Labrecque G and Bélanger PM (1991) Biological rhythms in the absorption, distribution, metabolism and excretion of drugs. *Pharmacol Ther* **52:**95–107.

Leibach FH and Ganapathy V (1996) Peptide transporters in the intestine and the kidney. *Annu Rev Nutr* **16:**99–119.

Lemmer B (1999) Chronopharmacokinetics: implications for drug treatment. *J Pharm Pharmacol* **51:**887–890.

Lemmer B and Labrecque G (1987) Chronopharmacology and chronotherapeutics: definitions and concepts. *Chronobiol Int* **4:**319–329.

Lemmer B and Nold G (1991) Circadian changes in estimated hepatic blood flow in healthy subjects. *Br J Clin Pharmacol* **32:**627–629.

Naruhashi K, Sai Y, Tamai I, Suzuki N, and Tsuji A (2002) Pept1 mRNA expression is induced by starvation and its level correlates with absorptive transport of cefadroxil longitudinally in the rat intestine. *Pharm Res (NY)* **19:**1417–1423.

Nielsen CU, Amstrup J, Steffansen B, Frokjaer S, and Brodin B (2001) Epidermal growth factor inhibits glycylsarcosine transport and hPepT1 expression in a human intestinal cell line. *Am J Physiol* **281:**G191–G199.

Ogihara H, Suzuki T, Nagamachi Y, Inui K, and Takata K (1999) Peptide transporter in the rat small intestine: ultrastructural localization and the effect of starvation and administration of amino acids. *Histochem J* **31:**169–174.

Okano T, Inui K, Maegawa H, Takano M, and Hori R (1986) H^+ coupled uphill transport of aminocephalosporins via the dipeptide transport system in rabbit intestinal brush-border membranes. *J Biol Chem* **261:**14130–14134.

Pan X, Terada T, Irie M, Saito H, and Inui K (2002) Diurnal rhythm of H^+-peptide cotransporter in the rat small intestine. *Am J Physiol* **283:**G57–G64.

Rhoads DB, Rosenbaum DH, Unsal H, Isselbacher KJ, and Levitsky LL (1998) Circadian periodicity of intestinal Na^+/glucose cotransporter 1 mRNA levels is transcriptionally regulated. *J Biol Chem* **273:**9510–9516.

Saito H, Okuda M, Terada T, Sasaki S, and Inui K (1995) Cloning and characterization of a rat H^+/peptide cotransporter mediating absorption of β-lactam antibiotics in the intestine and kidney. *J Pharmacol Exp Ther* **275:**1631–1637.

Saito H, Terada T, Okuda M, Sasaki S, and Inui K (1996) Molecular cloning and tissue distribution of rats peptide transporter PEPT2. *Biochim Biophys Acta* **1280:**173–177.

Shen H, Smith DE, and Brosius FC 3rd (2001) Developmental expression of PEPT1 and PEPT2 in rat small intestine, colon and kidney. *Pediatr Res* **49:** 789–795.

Shiraga T, Miyamoto K, Tanaka H, Yamamoto H, Taketani Y, Morita K, Tamai I, Tsuji A, and Takeda E (1999) Cellular and molecular mechanisms of dietary regulation on rat intestinal H^+/peptide transporter PepT1. *Gastroenterology* **116:** 354–362.

Stevenson NR and Fierstein JS (1976) Circadian rhythms of intestinal sucrase and glucose transport: cued by time of feeding. *Am J Physiol* **230:**G731–G735.

Thamotharan M, Bawani SZ, Zhou X, and Adibi SA (1999) Hormonal regulation of oligopeptide transporter PEPT1 in a human intestinal cell line. *Am J Physiol* **276:**C821–C826.

Yamaguchi H, Yano I, Saito H, and Inui K (2002) Pharmacokinetic role of P-glycoprotein in oral bioavailability and intestinal secretion of grepafloxacin in vivo. *J Pharmacol Exp Ther* **300:**1063–1069.

Address correspondence to: Professor Ken-ichi Inui, Department of Pharmacy, Kyoto University Hospital, Sakyo-ku, Kyoto 606-8507, Japan. E-mail: inui@kuhp.kyoto-u.ac.jp

Drug Metab. Pharmacokin. 18 (6): 409-412 (2003).

Short Communication

Decreased Function of Genetic Variants, Pro283Leu and Arg287Gly, in Human Organic Cation Transporter hOCT1

Ayako TAKEUCHI, Hideyuki MOTOHASHI, Masahiro OKUDA and Ken-ichi INUI

Department of Pharmacy, Kyoto University Hospital, Kyoto, Japan

Summary: We have evaluated the functional consequences of genetic variations in human organic cation transporter hOCT1 (*SLC22A1*). Three coding single nucleotide polymorphisms (cSNPs) resulted in the amino acid changes Pro283Leu, Arg287Gly and Pro341Leu were assessed. Uptake experiments with transient expression system using HEK293 cells revealed that the variants Pro283Leu and Arg287Gly had completely diminished transport activity. The other variant Pro341Leu had a significantly, but not completely, decreased transport activity. Western blot analysis showed that the expression levels of all three variant proteins in the crude membranes of HEK293 cells were comparable to those of wild type hOCT1. Moreover, the expression of variant proteins at the plasma membrane was confirmed by indirect immunofluorescence, indicating that these SNPs did not affect the membrane localization of hOCT1. Present results suggest that the amino acid residues Pro283 and Arg287 have a substantial role in substrate recognition of hOCT1.

Key words: organic cation transporter; human; single nucleotide polymorphism; HEK293; tetraethylammonium; localization

Introduction

It has become apparent that some interindividual differences in drug disposition and response to drugs are caused by genetic variations in metabolizing enzymes and drug transporters.[1,2] The most abundant form of genetic variation is the single nucleotide polymorphism (SNP). In particular, SNP in coding regions of genes (cSNP) may alter the function or structure of the encoded proteins. Although recent advances in high-throughput screening methods permit a systematic detection of genetic variation in specific transporter genes and a construction of several SNP databases, the resulting functional consequences and phenotypes at the clinical stage remain to be defined in many cases.

Human organic cation transporter hOCT1 (*SLC22A1*) is a member of the organic ion transporter family cloned from human liver.[3,4] OCT1 mediates electrogenic transport of various cations including model compounds tetraethylammonium (TEA) and N^1-methylnicotinamide, as well as the neurotoxin 1-methyl-4-phenylpyridinium (MPP).[5,6] Recently, identification and functional consequences of several SNPs in *SLC22A1* have been reported.[7,8] However, some cSNPs in *SLC22A1* gene have yet been uncharacterized. In the present study, we selected three cSNPs, resulting in the amino acid changes Pro283Leu, Arg287Gly and Pro341Leu, from a public SNP database NCBI dbSNP (http://www.ncbi.nlm.nih.gov/SNP/).[9] We demonstrated for the first time the functional ablation of Pro283Leu and Arg287Gly variants despite a conserved protein expression at plasma membrane, together with a relatively preserved transport activity of Pro341Leu variant.

Materials and Methods

Materials: [ethyl-1-^{14}C]TEA (55 mCi/mmol) was purchased from American Radiolabeled Chemicals (St. Louis, MO). Unlabeled TEA was obtained from Nacalai Tesque (Kyoto, Japan). MPP was from Sigma Chemical Co. (St. Louis, MO). All other chemicals used were of the highest purity available.

cDNA cloning of human organic cation transporter: The full-length hOCT1 cDNA was isolated from a human liver Rapid-Screen™ Arrayed cDNA Library Panel (Origene™ Technologies inc, Rockville, MD),

This work was supported by a Grant-in-Aid for Research on Human Genome, Tissue Engineering, and Food Biotechnology from Ministry of Health, Labor and Welfare of Japan (H12-Genome-019) and a Grant-in-Aid for Scientific Research from Ministry of Education, Culture, Sports, Science and Technology of Japan. This work was carried out in collaboration with a PharmaSNP consortium.

Received; September 12, 2003, Accepted; October 24, 2003

To whom correspondence should be addressed: Prof. Ken-ichi INUI, Ph.D., *Department of Pharmacy, Kyoto University Hospital, Sakyo-ku, Kyoto 606-8507, Japan. Tel. +81-75-751-3577, Fax. +81-75-751-4207, E-mail: inui@kuhp.kyoto-u.ac.jp*

according to the manufacturer's protocols. That is, the library was screened by PCR using the following hOCT1-specific primers derived from the published sequence (Genbank accession number U77086): forward 5′-TGAGCATGCTGAGCCATCATG (bases 88 to 108) and reverse 5′-GAGCCAAAGAAGAAGCCCGCA (bases 593 to 573).

Construction of variants: The QuikChange™ site-directed mutagenesis kit (Stratagene, La Jolla, CA) was used to construct mutant cDNAs following the manufacturer's protocols. Three single point mutations (C/T953, C/G964 and C/T1127 corresponding to Pro283Leu, Arg287Gly and Pro341Leu, respectively) were introduced into hOCT1 cDNA. The nucleotide sequences of mutants were confirmed using a multicapillary DNA sequencer RISA384 system (Shimadzu, Kyoto, Japan).

Cell culture, transfection and uptake experiments: HEK293 cells were cultured as described previously.[10] pCMV6-XL4 plasmid vector DNA containing wild type hOCT1 and its variants were purified using Marligen High Purity Plasmid Purification Midiprep System (Marligen Bioscience, Ijamsville, MD). Transfection procedures and uptake experiments were performed as described previously.[10]

Western blot analysis: Crude plasma membrane fractions (1 μg) of HEK293 cells transiently transfected with vector alone, hOCT1 and its variants cDNAs were solubilized in loading buffer (2% SDS, 125 mM Tris-HCl, 20% glycerol, 50 mM dithiothreitol), heated at 95°C for 5 min, and Western blot analysis was performed as described previously.[11] To confirm the specificity of the antibody, the antibody was absorbed with an excess amount of antigen peptide (5 μg/mL) used as an immunogen.

Indirect immunofluorescence: HEK293 cells were seeded onto poly-L-lysine coated cover glasses (Matsunami Glass Ind., Ltd., Osaka, Japan) and then transfection was performed. Cells were fixed for 1 hr with acetone at −20°C. After being incubated with PBS containing 0.2% gelatin twice for 5 min, they were incubated with the anti-hOCT1 (1:200) for 1 hr at room temperature. Thereafter, cells were incubated with the Cy3 AffiniPure Goat Anti-Rabbit IgG (H + L) (Jackson ImmunoResearch Laboratories, Inc., West Grove, PA) at 1:100. These samples were examined with a BX-50-FLA fluorescence microscope (Olympus, Tokyo, Japan). Images were captured with a DP-50 CCD camera (Olympus) using Studio Lite software (Olympus).

Statistical analysis: Data were analyzed statistically using one-way analysis of variance followed by Fisher's t test.

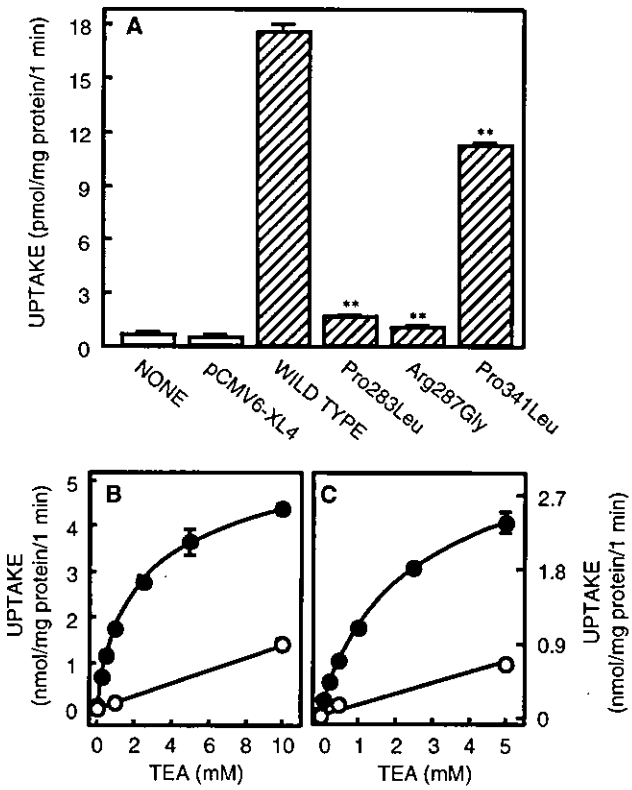

Fig. 1. A, Uptake of [^{14}C]TEA by HEK293 cells transiently transfected with vector alone, wild type hOCT1 and its variants cDNAs. HEK293 cells (NONE) and cells transfected with vector alone (pCMV6-XL4), wild type hOCT1 (WILD TYPE) and its variants (Pro283Leu, Arg287Gly and Pro341Leu) cDNAs were incubated with 5 μM of [^{14}C]TEA for 1 min at 37°C. Each column represents the mean ± SEM for three monolayers. **, $p < 0.01$, significant differences from WILD TYPE.

B, C, Dose-dependent uptake of [^{14}C]TEA by HEK293 cells transiently transfected with wild type hOCT1 (B) and its variant Pro341Leu (C) cDNAs.

Cells transfected with wild type hOCT1 (WILD TYPE) and Pro341Leu cDNAs were incubated for 1 min at 37°C with various concentrations of [^{14}C]TEA in the absence (closed circles) or presence (open circles) of 5 mM unlabeled MPP. Each point represents the mean ± SEM for three monolayers. When the *error bars* are not shown, they are smaller than the *symbol*.

Results and Discussion

In the present study, a complete functional ablation of two cSNPs Pro283Leu and Arg287Gly was shown for the first time (**Fig. 1A**). In contrast, another variant Pro341Leu exhibited a reduced but relatively preserved transport activity of [^{14}C]TEA. The uptake of TEA by wild type hOCT1 and Pro341Leu variant was saturated at high concentrations and was inhibited by the excess amount of MPP (**Figs. 1B, 1C**). Three separate experiments were performed to obtain the kinetic parameters and both *Km* value and *Vmax* value for Pro341Leu revealed to be significantly different from those of wild type hOCT1 (*Km*; 1.27 ± 0.09 mM for wild type and

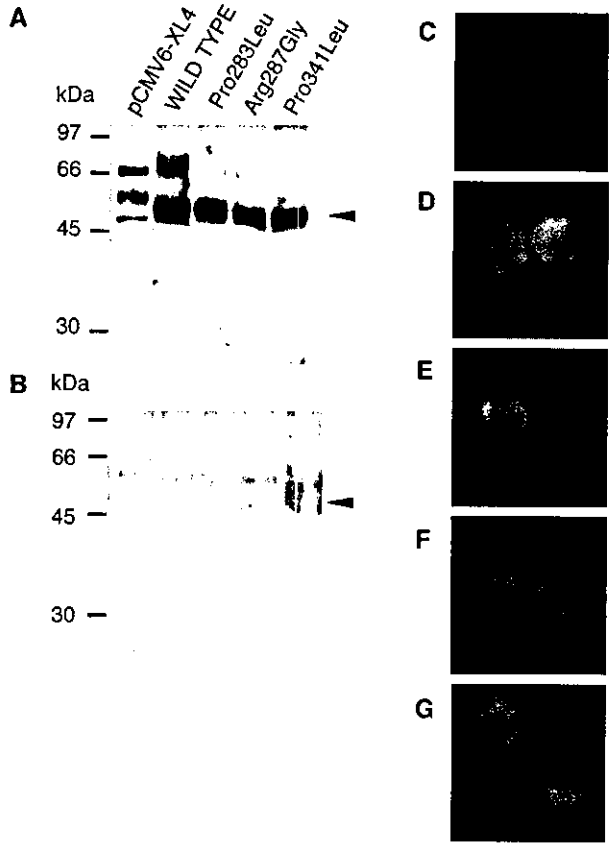

Fig. 2. A, B, Western blot analysis of crude membrane fractions obtained from HEK293 cells transiently transfected with vector alone, wild type hOCT1 and its variant cDNAs.
Crude membrane fractions (1 μg) obtained from HEK293 cells transiently transfected with vector alone (pCMV6-XL4), wild type hOCT1 (WILD TYPE) and its variants (Pro283Leu, Arg287Gly and Pro341Leu) cDNAs were separated by SDS-PAGE (10%) and blotted onto PVDF membranes. The antiserum for hOCT1 (1:2000) was used as primary antibody without (A) or with (B) the antigen peptide (5 μg/mL) of hOCT1. A horseradish peroxydase-conjugated anti-rabbit IgG antibody was used for detection of bound antibodies, and the strips of blots were visualized by chemiluminescence on X-ray film. The arrowhead indicates the position of hOCT1.
C-G, Localization of hOCT1 proteins in HEK293 cells transiently transfected with vector alone (C), wild type hOCT1 (D), its variants Pro283Leu (E), Arg287Gly (F) and Pro341Leu (G).
HEK293 cells transfected with vector alone, wild type hOCT1 and its variants (Pro283Leu, Arg287Gly and Pro341Leu) cDNAs were fixed and stained with antiserum for hOCT1. The magnification for each photo is ×200.

0.87±0.05 mM for Pro341Leu, $p<0.05$; *Vmax*; 4.09±0.29 nmol/mg protein/1 min for wild type and 1.79±0.15 nmol/mg protein/1 min for Pro341Leu, $p<0.01$). These results were consistent with a study using [^{3}H]MPP as substrate in an oocyte expressing system.[8]

To examine whether expression of hOCT1 proteins are altered in HEK293 cells expressing variants, we performed Western blot analysis. As shown in **Fig. 2A**, the immunoreactive protein was similarly detected in the cells transfected with wild type hOCT1 and its variants cDNAs, but not vector alone, indicating the conserved protein expressions. These positive bands disappeared when the antiserum was preabsorbed with the hOCT1 antigen peptide (**Fig. 2B**). Moreover, the localization of Pro283Leu and Arg287Gly variants were maintained at plasma membranes, in spite of the diminished TEA uptake (**Figs. 2C–2G**). In a previous study, a nonfunctional variant of *SLC22A1*, Gly465Arg, exhibited a reduced localization at the basolateral surface, suggesting a defect in membrane trafficking.[8] Accordingly, mechanism(s) other than decreased levels of protein expression or alterations in membrane localization, such as substrate recognition, would likely be responsible for the reduced transport function. Considering that the region between Pro283 and Leu289, located in the large intracellular loop between the predicted 6th and 7th transmembrane domains, is highly conserved among members of the organic cation transporter family,[5] this region may have a substantial role in the transport function in hOCT1.

At present, there is no report about the *in vivo* phenotypes of functionally deleterious mutations in the *SLC22A1* gene. Recently, decreased distributions in the liver of an anticancer drug metaiodobenzylguanidine and an antidiabetic drug metformin have been reported in *Oct1* knockout mice.[12,13] Therefore, large clinical studies on the genotype-phenotype relationship, using substrates of hOCT1 such as metformin, would provide a useful information about the contribution of *SLC22A1* gene polymorphisms in the individuals.

In conclusion, we demonstrated the functional consequences of Pro283Leu and Arg287Gly variants for the first time. In addition, this is the first report that represents the functional ablation of *SLC22A1* variants in spite of their normal expression at the plasma membranes. Further study should be needed to clarify whether these SNPs in *SLC22A1* may contribute to the interindividual variability in the disposition of several endogenous and exogenous cationic compounds.

References

1) Evans, W. E. and Relling, M. V.: Pharmacogenomics: Translating functional genomics into rational therapeutics. *Science*, **286**: 487–491 (1999).
2) Pauli-Magnus, C. and Meier, P. J.: Pharmacogenetics of hepatocellular transporters. *Pharmacogenetics*, **13**: 189–198 (2003).
3) Zhang, L., Dresser, M. J., Gray, A. T., Yost, S. C., Terashita, S. and Giacomini, K. M.: Cloning and functional expression of a human liver organic cation transporter. *Mol. Pharmacol.*, **51**: 913–921 (1997).
4) Gorboulev, V., Ulzheimer, J. C., Akhoundova, A., Ulzheimer-Teuber, I., Karbach, U., Quester, S., Baumann, C., Lang, F., Busch, A. E. and Koepsell, H.: Cloning and characterization of two human polyspecific organic cation transporters. *DNA Cell Biol.*, **16**: 871–881

(1997).
5) Koepsell, H.: Organic cation transporters in intestine, kidney, liver, and brain. *Annu. Rev. Physiol.*, **60**: 243-266 (1998).
6) Inui, K., Masuda, M. and Saito, H.: Cellular and molecular aspects of drug transport in the kidney. *Kidney Int.*, **58**: 944-958 (2000).
7) Kerb, R., Brinkmann, U., Chatskaia, N., Gorbunov, D., Gorboulev, V., Mornhinweg, E., Keil, A., Eichelbaum, M. and Koepsell, H.: Identification of genetic variations of the human organic cation transporter hOCT1 and their functional consequences. *Pharmacogenetics*, **12**: 591-595 (2002).
8) Shu, Y., Leabman, M. K., Feng, B., Mangravite, L. M., Huang, C. C., Stryke, D., Kawamoto, M., Johns, S. J., DeYoung, J., Carlson, E., Ferrin, T. E., Herskowitz, I. and Giacomini, K. M.: Evolutionary conservation predicts function of variants of the human organic cation transporter, OCT1. *Proc. Natl. Acad. Sci. USA*, **100**: 5902-5907 (2003).
9) Saito, S., Iida, A., Sekine, A., Ogawa, C., Kawauchi, S., Higuchi, S. and Nakamura, Y.: Catalog of 238 variations among six human genes encoding solute carriers (hSLCs) in the Japanese population. *J. Human Genet.*, **47**: 576-584 (2002).
10) Urakami, Y., Akazawa, M., Saito, H., Okuda, M. and Inui, K.: cDNA cloning, functional characterization, and tissue distribution of an alternatively spliced variant of organic cation transporter hOCT2 predominantly expressed in the human kidney. *J. Am. Soc. Nephrol.*, **13**: 1703-1710 (2002).
11) Motohashi, H., Sakurai, Y., Saito, H., Masuda, S., Urakami, Y., Goto, M., Fukatsu, A., Ogawa, O. and Inui, K.: Gene expression levels and immunolocalization of organic ion transporters in the human kidney. *J. Am. Soc. Nephrol.*, **13**: 866-874 (2002).
12) Jonker, J. W., Wagenaar, E., Mol, C. A. A. M., Buitelaar, M., Koepsell, H., Smit, J. W. and Schinkel, A. H.: Reduced hepatic uptake and intestinal excretion of organic cations in mice with a targeted disruption of the organic cation transporter 1 (Oct1 [Slc22a1]) gene. *Mol. Cell. Biol.*, **21**: 5471-5477 (2001).
13) Wang, D. S., Jonker, J. W., Kato, Y., Kusuhara, H., Schinkel, A. H. and Sugiyama, Y.: Involvement of organic cation transporter 1 in hepatic and intestinal distribution of metformin. *J. Pharmacol. Exp. Ther.*, **302**: 510-515 (2002).

Pharmaceutical Research, Vol. 21, No. 1, January 2004 (© 2004) *Research Paper*

Expression Levels of Renal Organic Anion Transporters (OATs) and Their Correlation with Anionic Drug Excretion in Patients with Renal Diseases

Yuji Sakurai,[1] Hideyuki Motohashi,[1] Harumasa Ueo,[1] Satohiro Masuda,[1] Hideyuki Saito,[1] Masahiro Okuda,[1] Noriko Mori,[2] Motokazu Matsuura,[3] Toshio Doi,[3] Atsushi Fukatsu,[4] Osamu Ogawa,[5] and Ken-ichi Inui[1,6]

Received August 2, 2003; accepted September 19, 2003

Purpose. Because the urinary excretion of drugs is often decreased in renal diseases, dosage regimens are adjusted to avoid adverse drug reactions. The aim of present study was to clarify the alteration in the levels of renal drug transporters and their correlation with the urinary drug excretion in renal diseases patients.

Methods. We quantified the mRNA levels of human organic anion transporters (hOATs) by real-time polymerase chain reaction and examined the excretion of the anionic drug, cefazolin, in renal disease patients. Moreover, transport of cefazolin by hOAT1 and hOAT3 were examined using HEK293 transfectants.

Results. Among four hOATs, the level of hOAT1 mRNA was significantly lower in the kidney of patients with renal diseases than in the normal controls. The elimination constant of cefazolin showed a significant correlation with the values of phenolsulfonphthalein test and mRNA levels of hOAT3. The uptake study using HEK293 transfectants revealed that cefazolin and phenolsulfonphthalein were transported by hOAT3.

Conclusions. These results suggest that hOAT3 plays an important role for anionic drug secretion in patients with renal diseases and that the expression levels of drug transporters may be related to the alteration of renal drug secretion.

KEY WORDS: organic anion transporter; renal diseases; human kidney; renal tubular secretion; real-time PCR.

INTRODUCTION

Renal impairments often decrease the rate of drug excretion into urine, and optimal dosage regimens must be designed to avoid adverse effects. For many drugs which are eliminated by the kidney, dosage regimens are usually adjusted according to creatinine clearance with a simple equation (1). However, it is accepted that the creatinine clearance (CL_{cr}) reflects only the glomerular filtration rate of normal kidney, and there are some discrepancies between the true glomerular filtration rate and CL_{cr} in patients with renal insufficiency. In addition, numerous ionic drugs are secreted into urine by the transporters localized in the proximal tubules. Indeed, the dosage schedule based on CL_{cr} was inadequate for ampicillin and cephalexin dosing in some patients with renal insufficiency (2). The adjustment method of the cephalexin dosage regimen, in which CL_{cr} and phenolsulfonphthalein test were simultaneously considered, appeared to be more useful than the conventional CL_{cr} method (3). Most of the phenolsulfonphthalein excretion into urine depends on the tubular secretion mediated by the organic anion transport systems (4). Although the dosage adjustment method, considering the ability of renal tubular secretion, may be useful for patients with renal diseases, little information is available about the expression profiles of the organic ion transporters in renal diseases.

Both renal secretion and reabsorption across the tubular epithelium are mediated by various transporters, which are expressed in the apical and basolateral membranes of tubular epithelial cells (5–7). Human organic anion transporter hOAT1 was isolated from the kidney and was suggested to be the *p*-aminohippurate/dicarboxylate exchanger (8,9). We previously clarified that the expression level of hOAT1 was the second highest among the organic ion transporters (SLC22A) and that hOAT1 was located at the basolateral membrane of the proximal tubules (10). It was suggested that hOAT1 mediated the basolateral uptake into the epithelial cells from the blood circulation. Human (h)OAT2 was also expressed in the basolateral membrane of renal tubular epithelium (11). Human OAT3 was isolated from the kidney (12). The expression levels of hOAT3 mRNA was the highest among organic ion transporter family in the human kidney, and hOAT3 protein was detected in the basolateral membrane of the proximal tubules (10). Recently, Sweet *et al.* (13) established the Oat3 knockout mouse. Although the generated $Oat3^{-/-}$ mice were fertile and exhibited no obvious morphological defects, the uptake of taurocholate, estrone sulfate, and *p*-aminohippurate in renal slices prepared from $Oat3^{-/-}$ mice were greatly reduced in comparison with wild-type mice, suggesting OAT3 may play an important role for basolateral anion transport of the proximal tubules. Human OAT4 was also expressed in the kidney, whereas it was localized to the apical side of the proximal tubules (14). These hOATs mediate the transport of various drugs and contribute to the renal drug excretion (6).

The purpose of this study is to clarify the expression levels of renal hOATs in the patients with renal diseases and their correlation with the rate of the anionic drug elimination. We quantified the mRNA levels of renal organic anion transporters in the normal parts of kidney cortex from surgically nephrectomized patients and in the renal biopsy specimens from patients with renal diseases. In addition, elimination of the anionic drug, cefazolin was assessed to compare with the expression levels of renal transporters or the 15- or 120-min value of the phenolsulfonphthalein test (PSP15′ or PSP120′). The transport characteristics of phenolsulfonphthalein and cefazolin by HEK293 transfectants with hOAT1 or hOAT3 were also examined.

[1] Department of Pharmacy, Kyoto University Hospital, Faculty of Medicine, Kyoto University, Sakyo-ku, Kyoto 606-8507, Japan.
[2] Department of Nephrology, Shizuoka Prefectural Hospital, Shizuoka, Japan.
[3] Department of Clinical Biology and Medicine, University of Tokushima, Tokushima, Japan.
[4] Division of Artificial Kidneys, Kyoto University Hospital, Faculty of Medicine, Kyoto University, Sakyo-ku, Kyoto 606-8507, Japan.
[5] Department of Urology, Kyoto University Hospital, Faculty of Medicine, Kyoto University, Sakyo-ku, Kyoto 606-8507, Japan.
[6] To whom correspondence should be addressed. (e-mail: inui@kuhp.kyoto-u.ac.jp)

0724-8741/04/0100-0061/0 © 2004 Plenum Publishing Corporation

MATERIALS AND METHODS

Normal Parts of the Kidney Cortex and Renal Biopsy Samples

Normal parts of human kidney cortex were obtained from 35 surgically nephrectomized patients with renal cell carcinoma or transitional cell carcinoma at Kyoto University Hospital (24 males and 11 females; age, 64.1 ± 7.9 year [mean ± SD]). These patients did not have any diseases that affected the kidney other than the carcinoma. Human kidney biopsy samples for the diagnosis were from 42 patients with various renal diseases at Tokushima University Hospital and Shizuoka Prefectural Hospital (24 males and 18 females; age, 39.2 ± 19.3 year [mean ± SD]). The characteristics of these patients are summarized in Table I. The patients had various renal diseases that were histologically confirmed as lupus nephritis (n = 4), IgA nephropathy (n = 11), focal glomerular sclerosis (n = 4), membranoproliferative glomerulonephritis (n = 3), membranous glomerulonephropathy (n = 6), mesangial proliferative glomerulonephropathy (n = 8), and other nephropathies (n = 6). Kidney biopsy specimens were histologically confirmed to contain the cortical proximal tubules using the adjacent sections. The values of clinical tests, such as CL_{cr}, PSP15′, or PSP120′, were routinely measured in the hospital. After phenolsulfonphthalein (6 mg) was administered intravenously, urine samples were collected at 15 and 120 min. The amounts of phenolsulfonphthalein in urine samples were represented as % of the initial dose. This study was conducted in accordance with the Declaration of Helsinki and its amendments and was approved by Kyoto University Graduate School and Faculty of Medicine, Ethics Committee. All patients gave their written informed consent.

Quantification of Organic Anion Transporter mRNA Expression

The expression levels of the drug transporters were quantified as described previously (10). Briefly, total cellular RNA was isolated from specimens using a MagNA Pure LC RNA isolation Kit II (Roche Diagnostic GmbH, Mannheim, Germany) and was reverse-transcribed to yield cDNA. Real-time polymerase chain reaction (PCR) was performed using the ABI PRISM 7700 sequence detector system (Applied Biosystems, Foster, CA, USA). Glyceraldehyde-3-phosphate dehydrogenase (GAPDH) mRNA was also quantified as an internal control with GAPDH Control Reagent (Applied Biosystems).

Table I. Characteristics of the Patients

	Nephrectomized patients	Patients with renal diseases
Age (years)	64.1 ± 7.9	39.2 ± 19.3
Males/females	24/11	24/18
Aspartate aminotransferase (IU/l)	25.8 ± 16.3	19.4 ± 10.2
Alanine aminotransferase (IU/l)	25.8 ± 19.2	19.8 ± 21.5
Lactate dehydrogenase (IU/l)	190.4 ± 76.5	175.5 ± 44.8
Serum creatinine (mg/dl)	0.85 ± 0.22	1.3 ± 1.9
Uric acid (mg/dl)	5.4 ± 1.7	6.2 ± 1.7
Blood urea nitrogen (mg/dl)	15.2 ± 4.8	18.7 ± 13.9
Creatinine clearance (ml/min)	77.6 ± 25.8	58.8 ± 24.4

Calculation of the Apparent Elimination Constants and Renal Secretion of Cefazolin

After the renal biopsy, the patients received 1 g of cefazolin by 1 h intravenous infusion for the prophylaxis of infections. The blood samples of the patients were collected immediately and at 1 h after the infusion. To 100 μl of collected plasma, 200 μl of methanol and 50 μl of cefotiam (100 μg/ml), as an internal standard, were added. After standing for 1 h at room temperature, the mixtures were centrifuged and the supernatants were filtered through a Millipore filter (SJGVL, 0.45 μm, Bedford, MA, USA). The filtrate was analyzed using high-performance liquid chromatography (HPLC) as described below, and the apparent elimination constant (Ke_{cez}) was calculated using the plasma concentration at immediately and 1hr after cefazolin infusion. A high-performance liquid chromatography (LC-10AS, Shimadzu Co., Kyoto, Japan) equipped with a UV spectrophotometric detector (SPD-10AV, Shimadzu) was used for the analysis of cefazolin. The conditions were as follows: column, Zorbax ODS column 4.6 mm inside diameter × 150 mm (Du Pont, Wilmington, DE, USA); mobile phase, 30 mM phosphate buffer (pH 7.0):methanol = 80:20; flow rate, 1.0 ml/min; wavelength, 272 nm; injection volume, 50 μl; temperature, 40°C.

Uptake of *p*-Aminohippurate and Estrone Sulfate by HEK293 Cells Transfected with hOAT1 or hOAT3 cDNA, Respectively

Human OAT1 cDNA was isolated from TriplEX™ human kidney cDNA library (BD Biosciences Clontech, Palo Alto, CA, USA) and hOAT3 cDNA was from the Human Kidney Rapid-Screen™ cDNA Panel (OriGene Technologies, Rockville, MD, USA) according to the instruction manuals. Isolated cDNAs were sequenced using a fluorescence 373A DNA sequencer (Applied Biosystems), and were subcloned into pBK-CMV plasmid vector (Stratagene, La Jolla, CA, USA). Cell culture, transfection of cDNA, and uptake studies were performed as described previously (15) with some modifications. Briefly, the day before transfection, HEK293 cells were seeded on poly-D-lysine-coated 24-well plates at a density of 2×10^5 cells/well. The cells were transfected with plasmid cDNA using LipofectAMINE 2000 (Invitrogen, Carlsbad, CA, USA). At 48 h after transfection, the uptake of *p*-[^{14}C]aminohippurate or [^{3}H]estrone sulfate by the HEK293 cells was examined. The composition of the incubation medium was as follows (in mM): 145 NaCl, 3 KCl, 1 $CaCl_2$, 0.5 $MgCl_2$, 5 D-glucose, and 5 HEPES (pH 7.4). The cells were preincubated with 0.2 ml of incubation medium for 10 min at 37°C. After the preincubation, medium was replaced with 0.2 ml of the incubation medium containing 5 μM *p*-[^{14}C]aminohippurate or 18.8 nM [^{3}H]estrone sulfate. At the end of incubation period, the medium was aspirated, and then cells were washed two times with 1 ml of ice-cold incubation medium. The cells were lysed in 0.5 ml of 0.5 N NaOH solution, and the radioactivity in aliquots was determined in 5 ml of ACSII (Amersham International, Buckinghamshire, UK). The protein contents of the solubilized cells were determined by the method of Bradford (16) using the Bio-Rad Protein Assay kit (Bio-Rad, Hercules, CA, USA) with the bovine γ-globulin as a standard.

Uptake of Cefazolin and Phenolsulfonphthalein by HEK293 Cells Transfected with hOAT1 or hOAT3 cDNA

For the uptake study of cefazolin and phenolsulfonphthalein, HEK293 cells were seeded on 6-cm poly-D-lysine-coated dish at a density of 2×10^6 cells/dish and then transfected with 8 μg hOAT1 or hOAT3 cDNA per dish at 24 h after seeding. At 48 h after transfection, the uptake studies of cefazolin and phenolsulfonphthalein were performed. The cells were preincubated with 2 ml of incubation medium for 10 min. After the preincubation, the medium was replaced with 2 ml of the incubation medium containing 200 μM cefazolin or 500 μM phenolsulfonphthalein. At the end of the 1-h incubation period, the medium was aspirated, and cells were washed once with 5 ml of ice-cold incubation medium containing 2% bovine serum albumin, and then four times with bovine serum albumin free ice-cold incubation medium. For measurement of the cefazolin accumulation, the cells were scraped and homogenized with 1 ml water. With 5 μl of the homogenate, protein contents were determined. To 0.98 ml of the homogenate, 20 μl of phosphoric acid was added and mixed for 30 s, then the samples were loaded onto an Oasis HLB cartridge (Waters Corporation, Milford, MA, USA) preconditioned with 1 ml each of methanol and water. The column was then washed with 1 ml of 5% methanol and then cefazolin was eluted from the column by 1 ml of methanol. The eluate was evaporated to bare dryness at 45–50°C and resuspended in 200 μl of mobile phase buffer, and the solution was filtered through a 0.45-μm polyvinylidene fluoride filter. The concentration of cefazolin was measured with HPLC under the following conditions: mobile phase, 30 mM phosphate buffer (pH 5.2):methanol = 88:12; flow rate, 1.0 ml/min; wavelength, 272 nm; temperature, 40°C. For measurement of the phenolsulfonphthalein accumulation, the cells were scraped with 1.5 ml of 75% ethanol, incubated for 1 h at room temperature, and centrifuged at 3000g for 10 min. After centrifugation, 1 ml of the supernatant was alkalized with 100 μl of 1 N NaOH and the concentration of phenolsulfonphthalein was determined spectrophotometrically at 546 nm. The pellet was solubilized with 1 ml of 1 N NaOH and protein contents were determined.

Statistical Analysis

Data were analyzed statistically using nonpaired *t* test or the one-way analysis of variance followed by Scheffe's test.

Materials

p-[Glycyl-^{14}C]aminohippurate (1.9 GBq/mmol) was purchased from Du Pont-New England Nuclear Research Product (Boston, MA, USA). [6,7-^{3}H(N)]Estrone sulfate ammonium salt (1.9 TBq/mmol) was obtained from Perkin Elmer Life Sciences (Boston, MA, USA). Cefazolin (Fujisawa Pharmaceutical Co., Osaka, Japan) was from the source. All other chemicals used were of the highest purity available.

RESULTS

Quantification of hOAT1, hOAT2, hOAT3, and hOAT4 mRNA Levels in the Normal Human Kidney Cortex and Renal Biopsy Samples

To investigate the expression levels of renal organic anion transporters, we performed quantitative real-time PCR. Fig. 1 shows the mRNA levels of organic anion transporters in normal parts of the renal cortex or the renal biopsy specimens from patients with kidney diseases. Only the level of hOAT1 mRNA in the renal biopsy specimens was significantly lower than that in the normal control ($p < 0.05$). The level of hOAT3 mRNA was slightly decreased, although the levels of hOAT2 and hOAT4 mRNA were increased in biopsy sections compared with each mRNA level in the normal kidney (differences not significant).

Correlation Between the Elimination Rate of Cefazolin and PSP15′, PSP120′, CL_{cr}, or Expression Levels of Organic Anion Transporters

Fig. 2 shows the linear regression of Ke_{cez} against PSP15′ (A), PSP120′ (B), or CL_{cr} (C) and the relation between CL_{cr} and PSP15′ (D) or PSP120′ (E). Although we detected a poor correlation between Ke_{cez} and CL_{cr} ($r = 0.40$, $p < 0.05$), there was a good linear correlation between Ke_{cez} and PSP15′ ($r = 0.75$, $p < 0.01$) or PSP120′ ($r = 0.67$, $p < 0.01$). However, there was a poor correlation between CL_{cr} and PSP15′ ($r = 0.48$, $p < 0.05$) or PSP120′ ($r = 0.56$, $p < 0.01$).

Fig. 3 shows the correlation between the Ke_{cez} and mRNA levels of organic anion transporters. The levels of hOAT3 mRNA was significantly correlated with the Ke_{cez} ($r = 0.44$, $p < 0.05$), although there was no correlation between hOAT1, hOAT2, or hOAT4 mRNA levels and Ke_{cez}.

Characterization of Organic Anion Uptake in HEK293 Cells Transfected with hOAT1 or hOAT3 cDNA

Good linear correlation between Ke_{cez} and PSP15′ or PSP120′ suggested that both cefazolin and phenolsulfonphthalein were excreted via the same organic anion transporters in the renal tubules. Therefore, we investigated the effects of cefazolin or phenolsulfonphthalein on the hOAT1 and hOAT3 transport activities. The transport function of hOAT1 and hOAT3 was assessed by the uptake of *p*-[^{14}C]aminohippurate and [^{3}H]estrone sulfate in HEK293 cells, respectively. Fig. 4 shows the time course of *p*-aminohippurate or estrone sulfate uptake by hOAT1- or hOAT3-expressing HEK293 cells. The accumulations of *p*-aminohippurate and estrone

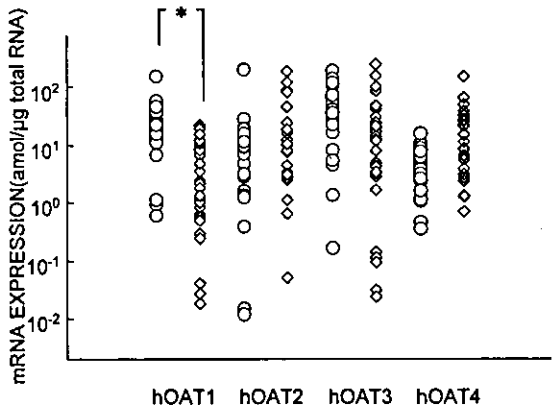

Fig. 1. Expression levels of hOAT1, hOAT2, hOAT3, and hOAT4 mRNA in the human kidney. Total cellular RNA was extracted from normal human kidney cortex (○) and renal biopsy specimens of patients with renal diseases (◇). The mRNA levels of these transporters were determined by real-time PCR. *$p < 0.05$, significant difference.

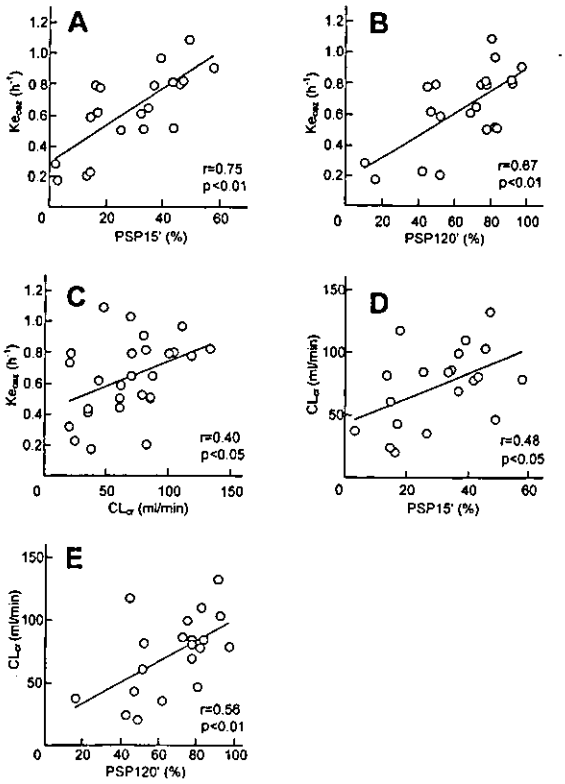

Fig. 2. The linear regression of the elimination constant of cefazolin against the 15- (A) or 120-min (B) values of the phenolsulfonphthalein test or creatinine clearance (C), and the relationship between creatinine clearance and 15- (D) or 120-min (E) values of the phenolsulfonphthalein test. The plasma concentration of cefazolin was measured by HPLC, and elimination constant of cefazolin (Ke_{cez}) was calculated.

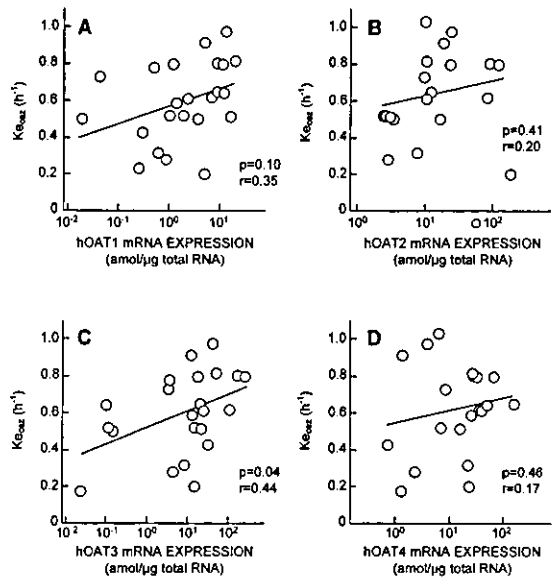

Fig. 3. The linear regression of Ke_{cez} against hOAT1 (A), hOAT2 (B), hOAT3 (C), and hOAT4 (D) mRNA levels. The plasma concentration of cefazolin was measured by HPLC, and Ke_{cez} was calculated. Total cellular RNA was extracted from the kidney biopsy specimens. The mRNA levels of hOAT1, hOAT2, hOAT3, and hOAT4 were quantified by real-time PCR.

sulfate were increased in a time-dependent manner, although the accumulations of these substrates in HEK293 cells, transfected with the blank vector alone, exhibited a negligible increase.

As shown in Fig. 5, a concentration-dependence of *p*-[^{14}C]aminohippurate and [^{3}H]estrone sulfate uptake was observed in hOAT1- and hOAT3-transfected cells. Using a nonlinear least squares regression analysis, kinetic parameters were calculated according to the Michaelis-Menten equation from three separate experiments. Apparent Michaelis-Menten constants (K_m) for *p*-[^{14}C]aminohippurate transport via hOAT1 and for [^{3}H]estrone sulfate transport via hOAT3 were 47.8 ± 19.5 and 6.6 ± 3.0 μM (mean ± SE), respectively, which were consistent with previous report (17). Maximal uptake rate (V_{max}) values for hOAT1 and hOAT3 were 305.7 ± 95.4 and 44.2 ± 8.1 pmol/mg protein/min (mean ± SE), respectively.

Fig. 6 shows that the effects of cefazolin or phenolsulfonphthalein on the hOAT1 or hOAT3 transport activity. Both cefazolin and phenolsulfonphthalein inhibited the organic anion uptake by hOAT1- and hOAT3-transfected cells, respectively, in a dose-dependent manner. The IC_{50} values were estimated by nonlinear regression analysis of the competition curves with one compartment model with the following equation: $V = 100 \times IC_{50} / (IC_{50} + [I]) + A$, where V is the uptake amount (% of control), $[I]$ is the concentration of cefazolin or phenolsulfonphthalein, and A is the nonspecific organic anion uptake (% of control). The IC_{50} values for cefazolin and phenolsulfonphthalein on hOAT1-mediated *p*-aminohippurate uptake were 100.6 ± 25.3 μM and 8.1 ± 1.3 μM, respectively, and the IC_{50} values for cefazolin and phenolsulfonphthalein on hOAT3-mediated estrone sulfate uptake were 116.6 ± 13.0 μM and 66.0 ± 16.5 μM, respectively.

Uptake of Cefazolin and Phenolsulfonphthalein by hOAT1- and hOAT3-Expressing HEK293 Cells

To investigate whether cefazolin and phenolsulfonphthalein are the substrates for hOAT1 and hOAT3, we measured the accumulation of cefazolin and phenolsulfonphthalein in hOAT1- and hOAT3-expressing HEK293 cells. The cefazolin accumulation in hOAT3-expressing HEK293 cells was significantly higher than that in control cells and the uptake of

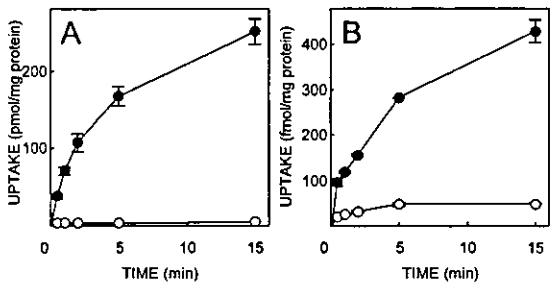

Fig. 4. Time course of *p*-[^{14}C]aminohippurate and [^{3}H]estrone sulfate accumulation in HEK293 cells. (A) *p*-[^{14}C]aminohippurate accumulation in HEK293 cells transfected with pBK-CMV vector (○) or hOAT1 (●) cDNA. The cells were incubated with 5 μM *p*-[^{14}C] aminohippurate at 37°C for specified periods. (B) [^{3}H] estrone sulfate accumulation in HEK293 cells transfected with pBK-CMV vector (○) or hOAT3 (●) cDNA. The cells were incubated with 18.8 nM [^{3}H]estrone sulfate at 37°C for specified periods. Each point represents the mean ± SE of three monolayers

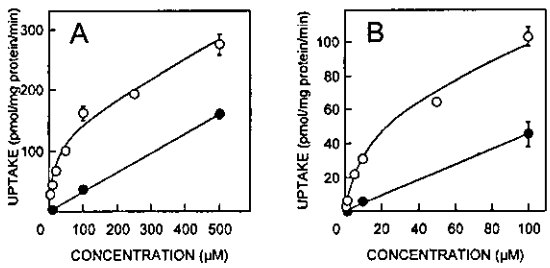

Fig. 5. Concentration dependence of *p*-[^{14}C]aminohippurate (A) and [^{3}H]estrone sulfate (B) accumulation in HEK293 cells transfected with hOAT1 or hOAT3 cDNA, respectively. The cells transfected with hOAT1 or hOAT3 cDNA were incubated with various concentrations of *p*-[^{14}C]aminohippurate (A) or [^{3}H]estrone sulfate (B) in the absence (○) or presence (●) of unlabeled 5 mM *p*-aminohippurate (A) or 1 mM estrone sulfate (B) at 37°C for 1 min. After incubation, radioactivity of solubilized cells was measured. Each point represents the mean ± SE of nine monolayers from three separate experiments.

cefazolin by hOAT3 was inhibited by phenolsulfonphthalein similar to the level of controls (Fig. 7A). In contrast, hOAT1-mediated cefazolin transport was not detected. We confirmed hOAT1-mediated *p*-aminohippurate uptake and hOAT3-mediated estrone sulfate uptake in the same transfected cells (Figs. 7B and C). As shown in Fig. 8, furthermore, the phenolsulfonphthalein accumulations in both hOAT1- and hOAT3-expressing HEK293 cells were significantly higher than those in control cells, and cefazolin inhibited the phenolsulfonphthalein uptake by both cells to the control level.

DISCUSSION

Renal secretion of various drugs is mediated by the drug transporters expressed in the tubular epithelial cells, and the alteration of these transporter levels may affect the drug elimination by the kidney. In the present study, the expression levels of organic anion transporters in kidney diseases were quantified to compare with those in normal controls, and then correlations between the mRNA levels of these transporters and anionic drug excretion were analyzed.

The mRNA level of hOAT1 in biopsy samples of patients with renal diseases was lower than that in the normal kidney cortex (Fig. 1). Although the level of hOAT3 mRNA also tended to decrease, the levels of hOAT2 and hOAT4 mRNA were apt to increase. Recently, we reported the alteration of the renal transporter expression in 5/6 nephrectomized rats, which have been widely used to study the progression of renal damage resulting from reduction of nephron mass (18–20). Rat organic cation transporter OCT2 protein was markedly decreased and H^+/peptide cotransporter PEPT2 protein was significantly increased in the kidney of these rats. Moreover, other transporters were not changed

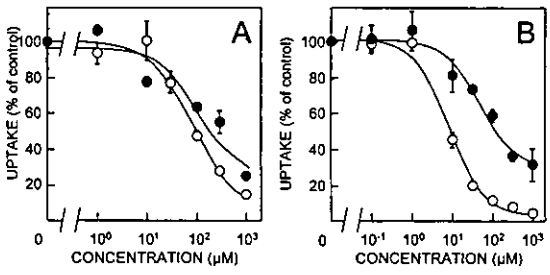

Fig. 6. Effects of cefazolin (A) or phenolsulfonphthalein (B) on *p*-[^{14}C]aminohippurate and [^{3}H]estrone sulfate accumulation in HEK293 cells transfected with hOAT1 or hOAT3 cDNA, respectively. Monolayers of hOAT1 (○)- or hOAT3 (●)-expressing HEK293 cells were incubated for 1 min at 37°C with 5 μM *p*-[^{14}C]aminohippurate (○) or 18.8 nM [^{3}H]estrone sulfate (●) in the presence of various concentrations of cefazolin or phenolsulfonphthalein. After incubation, the radioactivity of solubilized cells was measured. Each point represents the mean ± SE of nine monolayers from three separate experiments.

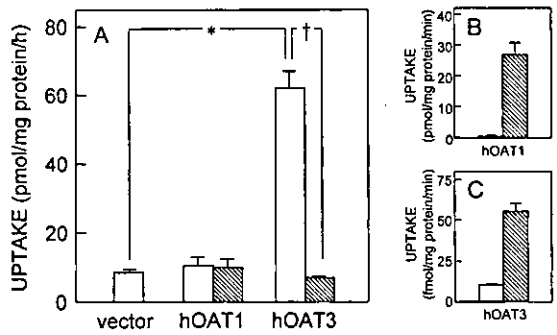

Fig. 7. Uptake of cefazolin in hOAT1 or hOAT3 transfected HEK293 cells. (A) Monolayers of hOAT1- or hOAT3-expressing HEK293 cells were incubated for 1 h at 37°C with 200 μM cefazolin in the absence (open columns) or presence (hatched columns) of 3 mM phenolsulfonphthalein. After incubation, the accumulation of cefazolin in the cells was measured by HPLC. (B) *p*-[^{14}C]aminohippurate accumulation in HEK293 cells transfected with pBK-CMV vector (open column) or hOAT1 (hatched column) cDNA. (C) [^{3}H]estrone sulfate accumulation in HEK293 cells transfected with pBK-CMV vector (open column) or hOAT3 (hatched column) cDNA. The cells were incubated with 5 μM *p*-[^{14}C]aminohippurate or 18.8 nM [^{3}H]estrone sulfate at 37°C for 1 min. Each column represents the mean ± SE of three monolayers. *p < 0.01, †p < 0.01, significant differences.

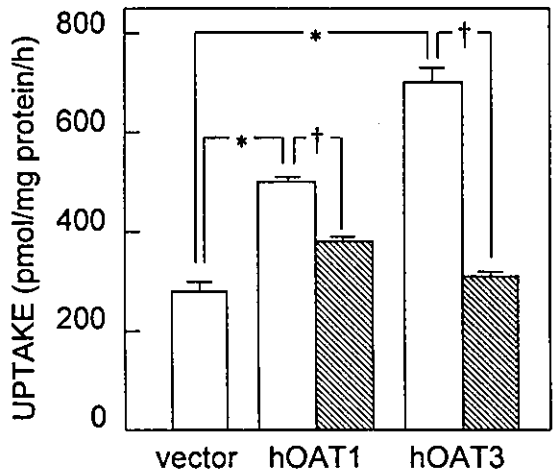

Fig. 8. Uptake of phenolsulfonphthalein in hOAT1 or hOAT3 transfected HEK293 cells. Monolayers of hOAT1- or hOAT3-expressing HEK293 cells were incubated for 1 h at 37°C with 500 μM phenolsulfonphthalein in the absence (open columns) or presence (hatched columns) of 10 mM cefazolin. After incubation, the accumulation of phenolsulfonphthalein in the cells was measured spectrophotometrically. Each column represents the mean ± SE of three monolayers. *p < 0.01, †p < 0.01, significant differences.

significantly. It was suggested that each transporter underwent a different effect in the impaired kidney.

In our previous study, we demonstrated that hOAT1 and hOAT3 could be major transporters in the human kidney cortex and localized at the basolateral membrane of the proximal tubular cells (10). Because hOAT1 and hOAT3 may play important roles in renal anion secretion, it was assumed that the changes in these expression levels affected renal drug secretion. In this study, cefazolin was selected to evaluate renal drug secretion, because it was reported that tubular secretion amounted to 50-80% of total excreted cefazolin in the patients with a glomerular filtration rate above 25 ml/min (21). In addition, the cefazolin elimination rate was significantly decreased by co-administration of probenecid to about 60% (22), suggesting that cefazolin was secreted by anion transport systems. Indeed, the Ke_{cez} varied among the patients. While no correlation could be found between the elimination rate of cefazolin (Ke_{cez}) and hOAT1, hOAT2 or hOAT4 expression levels, there is a significant correlation between Ke_{cez} and hOAT3 mRNA levels (Fig. 3). Although renal drug excretion is affected by many factors, such as glomerular filtration rate, renal blood flow rate, protein binding and transport abilities of tubular epithelial cells, the expression levels of transporters may be concerned mainly with transport capacities of epithelial cells. In addition, the patients in this study had various renal diseases and stages. Further investigation is needed to clarify more precise correlation between expression levels of transporters and renal drug secretion. So far, present results suggested that the renal excretion of the cefazolin was partly affected by hOAT3 expression levels.

The elimination rate of cefazolin was correlated with the urinary excretion of phenolsulfonphthalein (Fig. 2), suggesting that these compounds were excreted through common transporters. However, it was not certain which transporter mediated the secretion of these drugs in the human kidney. Phenolsulfonphthalein is mainly secreted from the kidney, and is often used for the diagnosis of renal function. It was reported that the accumulation of phenolsulfonphthalein into the renal tubules was inhibited by anionic compounds such as probenecid or 2,4-dinitrophenol (23). Therefore, tubular secretion of phenolsulfonphthalein should be mediated by the anion transport system (4). Hosoyamada *et al.* reported that phenolsulfonphthalein inhibited p-aminohippurate transport by hOAT1 (8). In this study, we confirmed that phenolsulfonphthalein inhibits the hOAT1-mediated *p*-aminohippurate transport in a dose-dependent manner. Moreover, it was shown that the phenolsulfonphthalein was transported by hOAT1 and hOAT3 (Fig. 8). Therefore, it is suggested that renal secretion of phenolsulfonphthalein is mediated by these transporters in the normal kidney.

It was reported that cefazolin inhibited the hOAT1- and hOAT3-mediated transport (24–26), and was transported by rOAT1 (27). In the present study, cefazolin inhibited the hOAT1- and hOAT3-mediated uptake, supporting previous finding. However, only hOAT3-mediated cefazolin transport could be detected in the present study (Fig. 7). Since this experiment was performed with higher concentration of cefazolin than IC_{50} value for cefazolin on hOAT1-mediated p-aminohippurate uptake, it could not be denied that cefazolin transport by hOAT1 should be detected at lower concentration. However, it is suggested that cefazolin is more effectively transported by hOAT3 than by hOAT1 and that hOAT3, rather than hOAT1, is the common transport pathway of tubular secretion of phenolsulfonphthalein and cefazolin.

The serum concentration of cefazolin at immediately after the infusion was 101.5 to 431.0 μM (data not shown). Because about 80% of cefazolin bound to the protein (21), the concentration of free serum cefazolin is comparable to IC_{50} value for cefazolin on hOAT3 transport. It is possible that cefazolin is efficiently transported by hOAT3 from blood circulation to tubular epithelial cells.

Patients with chronic renal insufficiency or nephritic syndrome frequently manifest diuretic resistance. It was suggested that the carrier-mediated tubular secretion of diuretics is important for its efficacy (28,29). In a previous study, we suggested that rOAT1 contributes, at least in part, to renal tubular secretion of acetazolamide, thiazides, and loop diuretics (30). In the present study, the hOAT1 mRNA level in the renal diseases was lower than that of normal parts of the kidney. It is possible that diuretic resistance may be partly due to the reduction of tubular secretion by the decreased hOAT1 expression.

This is the first report showing the expression profile of renal drug transporters in patients with kidney diseases and provided novel information as follows. Firstly, the hOAT1 mRNA levels in the kidney of patients with renal diseases were lower than in the normal kidney cortex. Secondly, renal excretion of the anionic drug cefazolin was significantly correlated with hOAT3 mRNA levels in patients with renal diseases. Thirdly, both phenolsulfonphthalein and cefazolin were transported by hOAT3. These results suggested that hOAT3 should play an important role on the secretion of these anionic drugs in patients with renal diseases. Although further investigation is needed to apply the expression levels of drug transporters to dosage adjustment, it is possible that the expression profiles of drug transporters may be useful information for understanding the alteration of renal drug secretion.

ACKNOWLEDGMENTS

This work was supported by a grant-in-aid for Research on Human Genome, Tissue Engineering and Food Biotechnology from the Ministry of Health, Labor and Welfare of Japan (H12-Genome-019) and a grant-in-aid for Scientific Research from the Ministry of Education, Culture, Sports, Science and Technology of Japan.

REFERENCES

1. L. Dettli. Drug dosage in renal disease. *Clin. Pharmacokinet.* 1:126–134 (1976).
2. R. Hori, K. Okumura, A. Kamiya, H. Nihira, and H. Nakano. Ampicillin and cephalexin in renal insufficiency. *Clin. Pharmacol. Ther.* 34:792–798 (1983).
3. R. Hori, K. Okumura, H. Nihira, H. Nakano, K. Akagi, and A. Kamiya. A new dosing regimen in renal insufficiency: application to cephalexin. *Clin. Pharmacol. Ther.* 38:290–295 (1985).
4. J. V. Moller and M. I. Sheikh. Renal organic anion transport system: pharmacological, physiological, and biochemical aspects. *Pharmacol. Rev.* 34:315–358 (1982).
5. G. Burckhardt and N. A. Wolff. Structure of renal organic anion and cation transporters. *Am. J. Physiol. Renal Physiol.* 278:F853–F866 (2000).

6. K. Inui, S. Masuda, and H. Saito. Cellular and molecular aspects of drug transport in the kidney. *Kidney Int.* **58**:944–958 (2000).
7. T. Sekine, S. H. Cha, and H. Endou. The multispecific organic anion transporter (OAT) family. *Pflugers Arch.* **440**:337–350 (2000).
8. M. Hosoyamada, T. Sekine, Y. Kanai, and H. Endou. Molecular cloning and functional expression of a multispecific organic anion transporter from human kidney. *Am. J. Physiol.* **276**:F122–F128 (1999).
9. R. Lu, B. S. Chan, and V. L. Schuster. Cloning of the human kidney PAH transporter: narrow substrate specificity and regulation by protein kinase C. *Am. J. Physiol.* **276**:F295–F303 (1999).
10. H. Motohashi, Y. Sakurai, H. Saito, S. Masuda, Y. Urakami, M. Goto, A. Fukatsu, O. Ogawa, and K. Inui. Gene expression levels and immunolocalization of organic ion transporters in the human kidney. *J. Am. Soc. Nephrol.* **13**:866–874 (2002).
11. A. Enomoto, M. Takeda, M. Shimoda, S. Narikawa, Y. Kobayashi, T. Yamamoto, T. Sekine, S. H. Cha, T. Niwa, and H. Endou. Interaction of human organic anion transporters 2 and 4 with organic anion transport inhibitors. *J. Pharmacol. Exp. Ther.* **301**: 797–802 (2002).
12. S. H. Cha, T. Sekine, J. Fukushima, Y. Kanai, Y. Kobayashi, T. Goya, and H. Endou. Identification and characterization of human organic anion transporter 3 expressing predominantly in the kidney. *Mol. Pharmacol.* **59**:1277–1286 (2001).
13. D. H. Sweet, D. S. Miller, J. B. Pritchard, Y. Fujiwara, D. R. Beier, and S. K. Nigam. Impaired organic anion transport in kidney and choroid plexus of organic anion transporter 3 (Oat3 (Slc22a8)) knockout mice. *J. Biol. Chem.* **277**:26934–26943 (2002).
14. E. Babu, M. Takeda, S. Narikawa, Y. Kobayashi, A. Enomoto, A. Tojo, S. H. Cha, T. Sekine, D. Sakthisekaran, and H. Endou. Role of human organic anion transporter 4 in the transport of ochratoxin A. *Biochim. Biophys. Acta* **1590**:64–75 (2002).
15. Y. Urakami, M. Akazawa, H. Saito, M. Okuda, and K. Inui. cDNA cloning, functional characterization, and tissue distribution of an alternatively spliced variant of organic cation transporter hOCT2 predominantly expressed in the human kidney. *J. Am. Soc. Nephrol.* **13**:1703–1710 (2002).
16. M. M. Bradford. A rapid and sensitive method for the quantitation of microgram quantities of protein utilizing the principle of protein-dye binding. *Anal. Biochem.* **72**:248–254 (1976).
17. M. Takeda, S. Narikawa, M. Hosoyamada, S. H. Cha, T. Sekine, and H. Endou. Characterization of organic anion transport inhibitors using cells stably expressing human organic anion transporters. *Eur. J. Pharmacol.* **419**:113–120 (2001).
18. K. Takahashi, S. Masuda, N. Nakamura, H. Saito, T. Futami, T. Doi, and K. Inui. Upregulation of H^+-peptide cotransporter PEPT2 in rat remnant kidney. *Am. J. Physiol. Renal Physiol.* **281**:F1109–F1116 (2001).
19. A. Takeuchi, S. Masuda, H. Saito, T. Doi, and K. Inui. Role of kidney-specific organic anion transporters in the urinary excretion of methotrexate. *Kidney Int.* **60**:1058–1068 (2001).
20. L. Ji, S. Masuda, H. Saito, and K. Inui. Down-regulation of rat organic cation transporter rOCT2 by 5/6 nephrectomy. *Kidney Int.* **62**:514–524 (2002).
21. E. K. Brodwall, T. Bergan, and O. Ørjavik. Kidney transport of cefazolin in normal and impaired renal function. *J. Antimicrob. Chemother.* **3**:585–592 (1977).
22. G. R. Brown. Cephalosporin-probenecid drug interactions. *Clin. Pharmacokinet.* **24**:289–300 (1993).
23. M. I. Sheikh. Renal handling of phenol red. I. A comparative study on the accumulation of phenol red and p-aminohippurate in rabbit kidney tubules in vitro. *J. Physiol.* **227**:565–590 (1972).
24. S. Jariyawat, T. Sekine, M. Takeda, N. Apiwattanakul, Y. Kanai, S. Sophasan, and H. Endou. The interaction and transport of β-lactam antibiotics with the cloned rat renal organic anion transporter 1. *J. Pharmacol. Exp. Ther.* **290**:672–677 (1999).
25. K. Y. Jung, M. Takeda, M. Shimoda, S. Narikawa, A. Tojo, K. Kim do, A. Chairoungdua, B. K. Choi, H. Kusuhara, Y. Sugiyama, T. Sekine, and H. Endou. Involvement of rat organic anion transporter 3 (rOAT3) in cephaloridine-induced nephrotoxicity: in comparison with rOAT1. *Life Sci.* **70**:1861–1874 (2002).
26. M. Takeda, E. Babu, S. Narikawa, and H. Endou. Interaction of human organic anion transporters with various cephalosporin antibiotics. *Eur. J. Pharmacol.* **438**:137–142 (2002).
27. Y. Uwai, H. Saito, and K. Inui. Rat renal organic anion transporter rOAT1 mediates transport of urinary-extreted cephalosporins, but not of biliary-extracted cefoperazon. *Drug. Metabol. Pharmacokin.* **17**:125–129 (2002).
28. M. Burg, L. Stoner, J. Cardinal, and N. Green. Furosemide effect on isolated perfused tubules. *Am. J. Physiol.* **225**:119–124 (1973).
29. J. F. Seely and J. H. Dirks. Site of action of diuretic drugs. *Kidney Int.* **11**:1–8 (1977).
30. Y. Uwai, H. Saito, Y. Hashimoto, and K. Inui. Interaction and transport of thiazide diuretics, loop diuretics, and acetazolamide via rat renal organic anion transporter rOAT1. *J. Pharmacol. Exp. Ther.* **295**:261–265 (2000).

Available online at www.sciencedirect.com
SCIENCE DIRECT®
Biochemical and Biophysical Research Communications 316 (2004) 416–420
BBRC
www.elsevier.com/locate/ybbrc

Genetic variant Arg57His in human H^+/peptide cotransporter 2 causes a complete loss of transport function

Tomohiro Terada, Megumi Irie, Masahiro Okuda, and Ken-ichi Inui*

Department of Pharmacy, Kyoto University Hospital, Sakyo-ku, Kyoto 606-8507, Japan

Received 11 February 2004

Abstract

We evaluated the functional consequences of genetic variations in human H^+/peptide cotransporter 2 (hPEPT2, *SLC15A2*) resulting in the amino acid changes Arg57His (R57H) and Pro409Ser (P409S). The transport activity of variant R57H was completely abolished, whereas that of variant P409S was comparable with that of wild-type hPEPT2 at pH 5.0–8.0. R57H variant protein was detected in the crude membranes of transiently expressed HEK293 cells by Western blot analysis. The expression of the R57H variant at the plasma membrane was confirmed by indirect immunofluorescence in *Xenopus* oocytes, suggesting that the loss of transport function of hPEPT2 R57H was not due to a change in membrane protein expression. This is the first demonstration of a functional impairment of the SLC15A family induced by a single nucleotide polymorphism.

Keywords: Peptide transporter; PEPT2; Single nucleotide polymorphism; HEK293; *Xenopus* oocytes

Drug transporters as well as drug-metabolizing enzymes play pivotal roles in determining the pharmacokinetic profiles of drugs and also their pharmacological effects. Recent technological advances such as massive molecular sequencing have allowed the identification of single nucleotide polymorphisms (SNPs) of drug transporters. Evans et al. [1,2] suggested that SNPs of drug transporter genes are responsible for the variation in drug responses among individuals. SNPs in coding regions (cSNPs) of drug transporters are of particular interest, because cSNPs induce amino acid mutations that may alter the function or membrane expression of drug transporters. The functional characterization of drug transporter cSNPs has been reported for human organic cation transporter 1 (hOCT1, *SLC22A1*) [3–5], hOCT2 (*SLC22A2*) [6], and human organic anion transporters (OATP-C (*SLC21A6*) and OATP-B (*SLC21A9*)) [7].

Human H^+/peptide cotransporter 2 (hPEPT2, *SLC15A2*), expressed in a variety of tissues including the kidney, lung, and brain, mediates the uphill transport of di- and tripeptides. In addition to small peptides, hPEPT2 can transport a wide variety of peptide-like drugs such as β-lactam antibiotics and some angiotensin converting enzyme inhibitors, because these drugs are structurally similar to small peptides [8,9]. Thus, hPEPT2 works not only as a nutritional transporter but also a drug transporter. In the public SNP database NCBI dbSNP (http://www.ncbi.nlm.nih.gov/SNP/), five cSNPs with nonsynonymous changes in *hPEPT2* are reported, but functional activities of variants induced by these cSNPs have not been characterized. In the present study, we selected two cSNPs in *hPEPT2*, resulting in the amino acid changes Arg57His (R57H) and Pro409Ser (P409S), and characterized their functional activities. We demonstrated for the first time the functional impairment of hPEPT2 R57H in spite of a conserved protein expression at the cell plasma membrane.

Materials and methods

Materials. [^{14}C]Glycylsarcosine (Gly-Sar) (4.07 GBq/mmol) was obtained from Moravek Biochemicals (Brea, CA).

cDNA cloning of hPEPT2. A human kidney cDNA library, which was kindly provided by Dr. T. Abe (Tohoku University Graduate

* Corresponding author. Fax: +81-75-751-4207.
E-mail address: inui@kuhp.kyoto-u.ac.jp (K.-i. Inui).

0006-291X/$ - see front matter © 2004 Elsevier Inc. All rights reserved.
doi:10.1016/j.bbrc.2004.02.063

School of Medicine), was screened by hybridization with hPEPT2 fragments labeled with [α-^{32}P]dCTP (3000 Ci/mmol; Amersham–Pharmcia Biotech, Uppsala, Sweden) as described previously [10]. pBluescript phagemid was excised from the Uni-Zap XR vector using a helper phage and the isolated clone possessed about a 4.5 kb insert. The full-length nucleotide sequences were analyzed using a multicapillary DNA sequencer RISA384 system (Shimadzu, Kyoto, Japan).

Construction of variants. The QuikChange site-directed mutagenesis kit (Stratagene, La Jolla, CA) was used to construct mutant cDNAs following the manufacturer's protocols using wild-type hPEPT2 cDNA inserted in the pBluescript vector as a template. The R57H (NCBI SNP ID: rs1316300) and P409S (NCBI SNP ID: rs1920305) in hPEPT2 were altered by G to A and by C to T mutations at nucleotide positions 207 and 1262, respectively (human PEPT2 reference sequence: NM_021082). The nucleotide sequences of mutants were confirmed using a multicapillary DNA sequencer RISA384 system (Shimadzu). These clones were then subcloned into the expression vector pcDNA3.1 (+) (Invitrogen, Carlsbad, CA).

Cell culture and transfection. HEK923 cells (American Type Culture Collection CRL-1573) were cultured as described previously [11,12]. pcDNA 3.1 (+) containing cDNA encoding wild-type hPEPT2 or its variants was transfected into HEK293 cells using Lipofect-AMINE 2000 Reagent (Invitrogen) according to the manufacturer's instructions. At 48 h after transfection, the cells were used for the uptake experiment and Western blot analysis.

Uptake experiment in HEK293 cells. Cellular uptake of [^{14}C]Gly-Sar was measured with monolayers grown on poly-D-lysine-coated 24-well plates. The incubation medium contained (millimolar) NaCl, 145; KCl, 3; $CaCl_2$, 1; $MgCl_2$, 0.5; D-glucose, 5, and 2-(*N*-morpholino)ethanesulfonic acid (MES), 5 (pH 6.0) or *N*-2-hydroxyethylpiperazine-*N'*-2-ethanesulfonic acid (Hepes), 5 (pH 7.4). The cells were preincubated with 0.2 mL incubation medium (pH 7.4) for 10 min at 37 °C. The medium was then removed and 0.2 mL of incubation medium (pH 6.0) containing [^{14}C]Gly-Sar was added. After 15 min incubation, the medium was aspirated, and the monolayers were rapidly washed twice with 1 mL of ice-cold incubation medium. The cells were solubilized in 0.5 mL of 0.5 N NaOH and then the radioactivity in aliquots was determined by liquid scintillation counting. The protein content of solubilized cells was determined by the method of Bradford [13] using a Bio-Rad Protein Assay Kit (Bio-Rad, Richmond, CA) with bovine γ-globulin as the standard.

Polyclonal antibody against hPEPT2. Polyclonal antibody was raised against a synthetic peptide corresponding to the intracellular domain near the COOH-terminal of hPEPT2 (KTEDMRGPADKH). The procedure for the preparation of polyclonal antibody was described previously [10].

Western blot analysis. The preparations of crude plasma membranes and procedures for Western blot analysis were also previously described [10,14]. To confirm the specificity of the antibody, the antibody was absorbed with an excess amount of antigen peptide (2 μg/ml) used as an immunogen, and Western blot analysis was carried out.

Functional expression in Xenopus oocytes. cRNA synthesis and uptake measurements were performed as described previously [14]. Indirect immunofluorescence microscopy for oocytes was performed as described [14]. Briefly, three days after injection, oocytes were fixed with 4% paraformaldehyde for 1 h, immersed in 30% sucrose for 18 h, embedded in O.C.T. compound (Sakura Finetechnical, Tokyo), and rapidly frozen at −20 °C. Sections (5 μm thick) were cut, blocked (10% goat serum), and incubated with the anti-hPEPT2 serum (1:500) for 1 h. Thereafter, sections were incubated with the Cy3 AffiniPure goat anti-rabbit IgG (H + L) at 1:100. These samples were examined with a BX-50-FLA fluorescence microscope (Olympus, Tokyo, Japan). Images were captured with a DP-50 CCD camera (Olympus) using Studio Lite software (Olympus).

Results

In the public SNP database NCBI dbSNP, five cSNPs are reported in the *SLC15A2* gene with nonsynonymous substitutions (R57H, L350F, P409S, R509K, and M704L). Recently, Leabman et al. [15] have reported that the evolutionary conservation of orthologous sequences was the best predictor of transporter function. As the sequences of human, rat, rabbit, and mouse PEPT2 were aligned, R57 and P409 were found to be conserved across the species, suggesting that alterations of these amino acids induced the functional change in hPEPT2. For other amino acid substitutions of hPEPT2, identical or similar amino acids were observed in other species. Thus, we focused on the hPEPT2 R57H and P409S variants and performed a functional characterization of them. The amino acids at positions 57 and 409 of hPEPT2 are shown in Fig. 1, which is based on the putative secondary structure model of Liu et al. [16].

First, we isolated hPEPT2 cDNA from the human kidney cDNA library. The isolated hPEPT2 cDNA was about 4.5 kb long, and the nucleotide sequence for the open reading frame was identical to that previously reported [16]. When the concentration dependence of [^{14}C]Gly-Sar uptake was examined, the K_m value of Gly-Sar was calculated at 170 μM (Fig. 2), which corresponds to reported values (74 μM) [17].

We then examined the transport activity of hPEPT2 R57H and P409S at pH 6.0. [^{14}C]Gly-Sar uptake by hPEPT2 P409S was not different from that by the wild type, whereas a complete loss of transport function of the hPEPT2 R57H variant was demonstrated (Fig. 3A). The same results were obtained in the *Xenopus* oocyte expression system (Fig. 3B).

To examine whether expression of hPEPT2 R57H is altered in HEK293 cells, Western blot analysis was performed. As shown in Fig. 4A, an immunoreactive protein with a molecular weight of about 90 kDa was detected in the cells transfected with wild-type hPEPT2 and its variants, but not vector alone. The expression

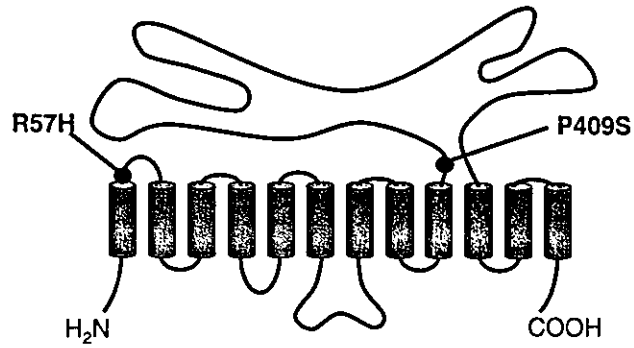

Fig. 1. hPEPT2 protein topology and the positions of the analyzed cSNP resulting in R57H and P409S.

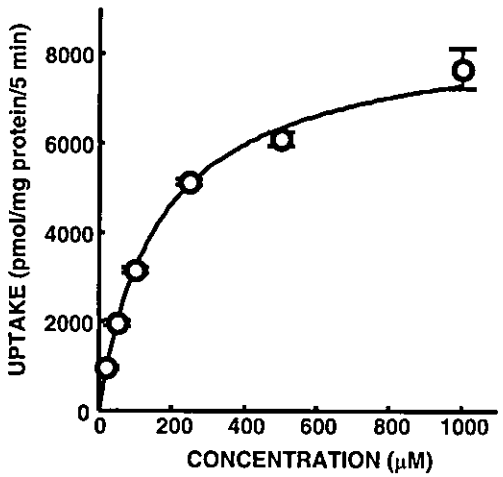

Fig. 2. Concentration dependence of [^{14}C]Gly-Sar uptake by HEK293 cells transiently expressing wild-type hPEPT2. HEK293 cells transfected with wild-type hPEPT2 were incubated with various concentrations of [^{14}C]Gly-Sar (pH 6.0) for 5 min at 37 °C. Each point represents the mean ± SE for three monolayers.

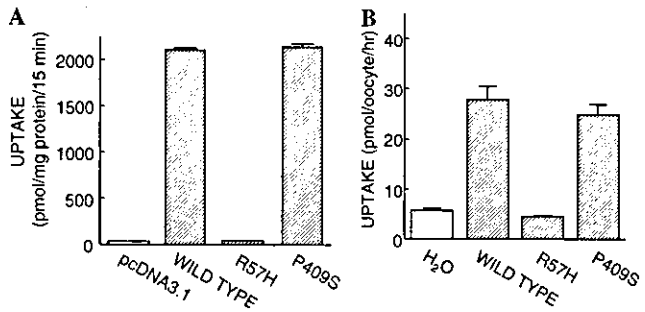

Fig. 3. [^{14}C]Gly-Sar uptake by HEK293 cells (A) and by oocytes (B) transiently expressing wild-type hPEPT2 and its variants R57H and P409S. (A) HEK293 cells transfected with vector alone (pcDNA3.1), wild-type hPEPT2 (wild type) and its variant (R57H and P409S) cDNA, were incubated with 20 μM [^{14}C]Gly-Sar (pH 6.0) for 15 min at 37 °C. Each column represents the mean ± SE for three monolayers. (B) Oocytes injected with H_2O, wild-type hPEPT2 and its variant (R57H and P409S) cRNA were incubated with 20 μM [^{14}C]Gly-Sar for 1 h at 25 °C. Each column represents the mean ± SE for 8 oocytes.

levels are comparable among the wild type and two variants. These positive bands disappeared when the antiserum was preabsorbed with the hPEPT2 antigen peptide (Fig. 4B). Furthermore, as shown in Fig. 5, the hPEPT2 R57H variant protein was expressed at plasma membranes as well as the wild type and P409S variant in the *Xenopus* oocyte expression system. These findings suggested that the loss of transport function of the hPEPT2 R57H variant was not due to a change in membrane protein expression.

The loss of transport function of hPEPT2 R57H may be caused by the differences in the charge of the side chain of arginine and histidine. The ratio of the non-protonated (neutral) to protonated (positive) side chain of arginine (side chain $pK_a = 12.5$) is 1:3,160,000 at pH 6.0, whereas that of histidine (side chain $pK_a = 6.0$) is

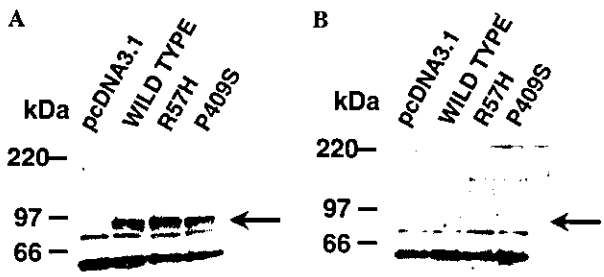

Fig. 4. Western blot analysis of crude membranes obtained from HEK293 cells transiently expressing with wild-type hPEPT2 and its variants R57H and P409S. Crude membranes (20 μg) obtained from HEK293 cells transiently transfected with vector alone (pcDNA3.1), wild-type hPEPT2 (wild type) and its variant (R57H and P409S) cDNAs were separated by SDS–PAGE (8.5%) and blotted onto PVDF membranes. The antiserum for hPEPT2 (1:500) was used as primary antibody without (A) or with (B) the antigen peptide (2 μg/ml) of hPEPT2. A horseradish peroxidase-conjugated anti-rabbit IgG antibody was used for detection of bound antibodies, and the strips of blots were visualized by chemiluminescence on X-ray film. The arrowhead indicates the position of hPEPT2.

1:1. Thus, we next measured the [^{14}C]Gly-Sar uptake at various pHs by the hPEPT2 wild type and two variants. As shown in Fig. 6, at all pH values tested, [^{14}C]Gly-Sar uptake by the wild type and P409S variant was comparable, whereas the transport activity of hPEPT2 R57H was completely lost.

Discussion

To date, there has been no report concerning the functional characterization of cSNPs of *SLC15A* genes. Here, we have demonstrated for the first time that an amino acid substitution (R57H) of hPEPT2 due to a cSNP caused a complete loss of transport function. According to recent studies in *Pept2* knockout mice, *Pept2*$^{-/-}$ mice were healthy and fertile, but dipeptide transport in the choroid plexus and kidney was reduced [18,19]. In addition to small peptides, Ocheltree et al. [20] have recently demonstrated that the uptake of cefadroxil, an oral β-lactam antibiotic, in the choroid plexus was reduced by 83% in *Pept2*$^{-/-}$ mice as compared to *Pept2*$^{+/+}$ mice, and suggested that PEPT2 is the primary transporter responsible for the choroid plexus uptake of peptide-like drugs at the blood–cerebrospinal fluid–barrier. If the findings in knockout mice can be extrapolated to humans, the homozygotes for this allele are healthy, but the handling of small peptides and peptide-like drugs in the choroid plexus and kidney may

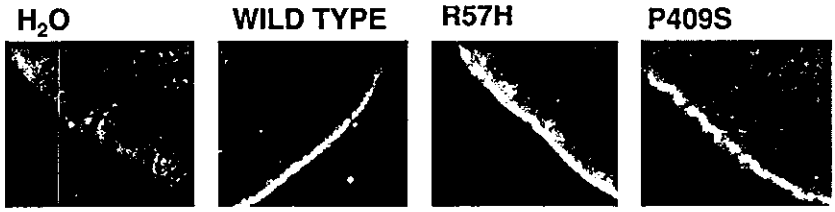

Fig. 5. Expression of wild-type hPEPT2 and its variant R57H and P409S in *Xenopus* oocytes. *Xenopus* oocytes injected with H_2O, wild-type hPEPT2 (wild type) and its variants (R57H and P409S) cRNAs were fixed and stained with antiserum for hPEPT2. Cy3-labeled anti-rabbit IgG was used for detection of bound antibodies.

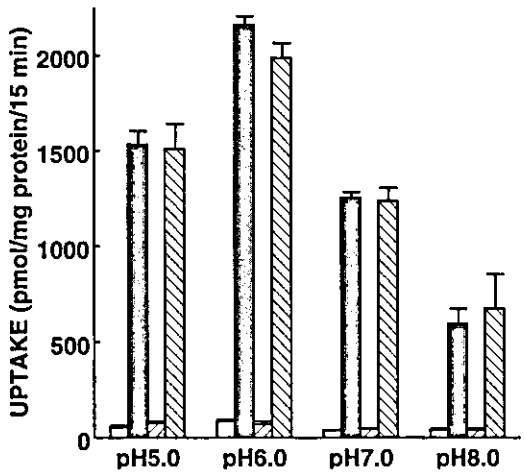

Fig. 6. pH-dependence of [^{14}C]Gly-Sar uptake by HEK293 cells transiently expressing wild-type hPEPT2 and its variants R57H and P409S. HEK293 cells transfected with vector alone (□), wild-type hPEPT2 (■), R57H (▨), and P409S (▧) cDNAs were incubated with 20 μM [^{14}C]Gly-Sar at various pHs for 15 min at 37 °C. Each column represents the mean ± SE for three monolayers.

be affected. Further clinical studies are needed to see whether this SNP affects the pharmacokinetic profiles of peptide-like drugs and might be responsible for inter-individual differences during drug therapy.

The present findings also provided significant information on the biology of H^+/peptide cotransporters. Interestingly, the critical amino acid residue Arg57 we identified is conserved in PEPT1 and PEPT2 across human, rat, rabbit, and mouse. Furthermore, recent functional analyses of chimeric PEPT1/PEPT2 proteins demonstrated that the N-terminal regions up to the second transmembrane domain (TMD) may form an important part of the peptide transporters [21]. As Arg57 is included in this region (Fig. 1), our data support the functional importance of this domain. What is the role of Arg residue at position 57 in hPEPT2? There have been several reports on the functional roles of the Arg residue in different transporters [22–24]. For example, in the lactose/H^+ symporter, Arg302 of this transporter facilitated the deprotonation of the carboxylic acid of Glu325 during the H^+ translocation process [23]. In the present study, we found that the R57H variant did not show transport activity at pH 5.0–8.0. It is noted that, at pH 5.0, the ratio of non-protonated to protonated side chain of histidine is 1:10, suggesting that the positive charge of the amino acid at position 57 did not compensate for the transport activity. Further studies are needed to determine the functional roles of Arg57 of hPEPT2.

Using site-directed mutagenesis, conserved His residues in the second and fourth TMDs of PEPT1 and PEPT2 were shown to be essential for the transport activity and/or substrate binding [14,25–27]. One His residue was suggested to be the binding site for the α-amino group of substrates [28] and the other a H^+-binding site [14,25–27]. Thus, there is the possibility that the loss of transport function in the R57H variant may be caused by interference of the His residue at position 57 by His residues located in the second and fourth TMDs of hPEPT2.

In conclusion, we demonstrated that the hPEPT2 R57H variant induced by cSNP G207A showed no transport activity in spite of a normal expression at the plasma membranes. These findings suggest that both peptide homeostasis and pharmacokinetic profiles of peptide-like drugs may be altered in homozygotes for this variant.

Acknowledgments

This work was supported by the 21st Century COE Program "Knowledge Information Infrastructure for Genome Science," a Grant-in-Aid for Comprehensive Research on Aging and Health from the Ministry of Health, Labor and Welfare of Japan, and a Grant-in-Aid for Scientific Research from the Ministry of Education, Culture, Sports, Science and Technology of Japan. This work was carried out in collaboration with a PharmaSNP consortium.

References

[1] W.E. Evans, M.V. Relling, Pharmacogenomics: translating functional genomics into rational therapeutics, Science 286 (1999) 487–491.
[2] W.E. Evans, H.L. McLeod, Pharmacogenomics—drug disposition, drug targets, and side effects, N. Engl. J. Med. 348 (2003) 538–549.
[3] R. Kerb, U. Brinkmann, N. Chatskaia, D. Gorbunov, V. Gorboulev, E. Mornhinweg, A. Keil, M. Eichelbaum, H. Koepsell, Identification of genetic variations of the human organic

cation transporter hOCT1 and their functional consequences, Pharmacogenetics 12 (2002) 591–595.
[4] Y. Shu, M.K. Leabman, B. Feng, L.M. Mangravite, C.C. Huang, D. Stryke, M. Kawamoto, S.J. Johns, J. DeYoung, E. Carlson, T.E. Ferrin, I. Herskowitz, K.M. Giacomini, Evolutionary conservation predicts function of variants of the human organic cation transporter, OCT1, Proc. Natl. Acad. Sci. USA 100 (2003) 5902–5907.
[5] A. Takeuchi, H. Motohashi, M. Okuda, K. Inui, Decreased function of genetic variants, Pro283Leu and Arg287Gly, in human organic cation transporter *hOCT1*, Drug Metab. Pharmacokinet. 18 (2003) 409–412.
[6] M.K. Leabman, C.C. Huang, M. Kawamoto, S.J. Johns, D. Stryke, T.E. Ferrin, J. DeYoung, T. Taylor, A.G. Clark, I. Herskowitz, K.M. Giacomini, Polymorphisms in a human kidney xenobiotic transporter, OCT2, exhibit altered function, Pharmacogenetics 12 (2002) 395–405.
[7] T. Nozawa, M. Nakajima, I. Tamai, K. Noda, J. Nezu, Y. Sai, A. Tsuji, T. Yokoi, Genetic polymorphisms of human organic anion transporters OATP-C (SLC21A6) and OATP-B (SLC21A9): allele frequencies in the Japanese population and functional analysis, J. Pharmacol. Exp. Ther. 302 (2002) 804–813.
[8] H. Daniel, I. Rubio-Aliaga, An update on renal peptide transporters, Am. J. Physiol. Renal Physiol. 284 (2003) F885–F892.
[9] K. Inui, T. Terada, Dipeptide transporters, in: G.L. Amidon, W. Sadée (Eds.), Membrane Transporters as Drug Targets, Kluwer Academic/Plenum Publishers, New York, 1999, pp. 269–288.
[10] H. Saito, M. Okuda, T. Terada, S. Sasaki, K. Inui, Cloning and characterization of a rat H^+/peptide cotransporter mediating absorption of β-lactam antibiotics in the intestine and kidney, J. Pharmacol. Exp. Ther. 275 (1995) 1631–1637.
[11] Y. Urakami, M. Akazawa, H. Saito, M. Okuda, K. Inui, cDNA cloning, functional characterization, and tissue distribution of an alternatively spliced variant of organic cation transporter hOCT2 predominantly expressed in the human kidney, J. Am. Soc. Nephrol. 13 (2002) 1703–1710.
[12] N. Horiba, S. Masuda, C. Ohnishi, D. Takeuchi, M. Okuda, K. Inui, Na^+-dependent fructose transport via rNaGLT1 in rat kidney, FEBS Lett. 546 (2003) 276–280.
[13] M.M. Bradford, A rapid and sensitive method for the quantitation of microgram quantities of protein utilizing the principle of protein-dye binding, Anal. Biochem. 72 (1976) 248–254.
[14] T. Terada, H. Saito, M. Mukai, K. Inui, Identification of the histidine residues involved in substrate recognition by a rat H^+/peptide cotransporter, PEPT1, FEBS Lett. 394 (1996) 196–200.
[15] M.K. Leabman, C.C. Huang, J. DeYoung, E.J. Carlson, T.R. Taylor, M. de la Cruz, S.J. Johns, D. Stryke, M. Kawamoto, T.J. Urban, D.L. Kroetz, T.E. Ferrin, A.G. Clark, N. Risch, I. Herskowitz, K.M. Giacomini, Natural variation in human membrane transporter genes reveals evolutionary and functional constraints, Proc. Natl. Acad. Sci. USA 100 (2003) 5896–5901.
[16] W. Liu, R. Liang, S. Ramamoorthy, Y.J. Fei, M.E. Ganapathy, M.A. Hediger, V. Ganapathy, F.H. Leibach, Molecular cloning of PEPT 2, a new member of the H^+/peptide cotransporter family, from human kidney, Biochim. Biophys. Acta 1235 (1995) 461–466.
[17] S. Ramamoorthy, W. Liu, Y.Y. Ma, T.L. Yang-Feng, V. Ganapathy, F.H. Leibach, Proton/peptide cotransporter (PEPT 2) from human kidney: functional characterization and chromosomal localization, Biochim. Biophys. Acta 1240 (1995) 1–4.
[18] H. Shen, D.E. Smith, R.F. Keep, J. Xiang, F.C. Brosius III, Targeted disruption of the PEPT2 gene markedly reduces dipeptide uptake in choroid plexus, J. Biol. Chem. 278 (2003) 4786–4791.
[19] I. Rubio-Aliaga, I. Frey, M. Boll, D.A. Groneberg, H.M. Eichinger, R. Balling, H. Daniel, Targeted disruption of the peptide transporter Pept2 gene in mice defines its physiological role in the kidney, Mol. Cell. Biol. 23 (2003) 3247–3252.
[20] S.M. Ocheltree, H. Shen, Y. Hu, J. Xiang, R.F. Keep, D.E. Smith, Mechanisms of cefadroxil uptake in the choroid plexus: studies in wild type and PEPT2 knockout mice, J. Pharmacol. Exp. Ther. 308 (2004) 462–467.
[21] F. Doring, C. Martini, J. Walter, H. Daniel, Importance of a small N-terminal region in mammalian peptide transporters for substrate affinity and function, J. Membr. Biol. 186 (2002) 55–62.
[22] X. Yao, A.M. Pajor, Arginine-349 and aspartate-373 of the Na^+/dicarboxylate cotransporter are conformationally sensitive residues, Biochemistry 41 (2002) 1083–1090.
[23] M. Sahin-Toth, H.R. Kaback, Arg-302 facilitates deprotonation of Glu-325 in the transport mechanism of the lactose permease from *Escherichia coli*, Proc. Natl. Acad. Sci. USA 98 (2001) 6068–6073.
[24] A. Bendahan, A. Armon, N. Madani, M.P. Kavanaugh, B.I. Kanner, Arginine 447 plays a pivotal role in substrate interactions in a neuronal glutamate transporter, J. Biol. Chem. 275 (2000) 37436–37442.
[25] Y.J. Fei, W. Liu, P.D. Prasad, R. Kekuda, T.G. Oblak, V. Ganapathy, F.H. Leibach, Identification of the histidyl residue obligatory for the catalytic activity of the human H^+/peptide cotransporters PEPT1 and PEPT2, Biochemistry 36 (1997) 452–460.
[26] X.Z. Chen, A. Steel, M.A. Hediger, Functional roles of histidine and tyrosine residues in the H^+-peptide transporter PepT1, Biochem. Biophys. Res. Commun. 272 (2000) 726–730.
[27] T. Uchiyama, A.K. Kulkarni, D.L. Davies, V.H.L. Lee, Biophysical evidence fro His^{57} as a proton-binding site in the mammalian intestinal transporter hPepT1, Pharm. Res. 20 (2003) 1911–1916.
[28] T. Terada, H. Saito, K. Inui, Interaction of β-lactam antibiotics with histidine residue of rat H^+/peptide cotransporters, PEPT1 and PEPT2, J. Biol. Chem. 273 (1998) 5582–5585.

J Hum Genet (2004) 49:40–45
DOI 10.1007/s10038-003-0105-4

ORIGINAL ARTICLE

Yuichi Uwai · Satohiro Masuda · Maki Goto
Hideyuki Motohashi · Hideyuki Saito
Masahiro Okuda · Eijirou Nakamura · Noriyuki Ito
Osamu Ogawa · Ken-ichi Inui

Common single nucleotide polymorphisms of the *MDR1* gene have no influence on its mRNA expression level of normal kidney cortex and renal cell carcinoma in Japanese nephrectomized patients

Received: 28 July 2003 / Accepted: 28 October 2003 / Published online: 18 December 2003

Abstract In this study, we have quantified the mRNA expression levels of multidrug resistance gene 1 (MDR1) in the normal kidney cortex and renal cell carcinoma (RCC) segments from 24 Japanese nephrectomized patients by real-time polymerase chain reaction (PCR). The mRNA expression level of MDR1 in RCC segments was significantly decreased in comparison with each normal segment ($P = 0.0042$, by Student's paired t-test). In addition, the ten common single nucleotide polymorphisms (SNPs) of the *MDR1* gene in the patients were assessed using the PCR-restriction enzyme fragment length polymorphism method to investigate the influence of these SNPs on its mRNA expression levels. The allele frequencies of these SNPs were comparable with our previous report in the Japanese recipients of living-donor liver transplantation (Goto et al., Pharmacogenetics 12:451–457; 2002). MDR1 expression levels in the normal kidney cortex were independent on the five SNPs, which were polymorphic in the Japanese population. Furthermore, the effect of the SNPs on expression levels of MDR1 mRNA in RCC segments was not recognized. These findings suggest that the common SNPs in the *MDR1* gene have no influence on the expression of its transcript in RCC segments as well as in the normal kidney cortex.

Keywords MDR1 · SNP · Kidney · Renal cell carcinoma

Y. Uwai · S. Masuda · M. Goto · H. Motohashi · H. Saito
M. Okuda · K. Inui (✉)
Department of Pharmacy, Kyoto University Hospital,
Sakyo-ku, Kyoto 606-8507, Japan
E-mail: inui@kuhp.kyoto-u.ac.jp
Tel.: +81-75-7513577
Fax: +81-75-7514207

E. Nakamura · N. Ito · O. Ogawa
Department of Urology, Graduate School of Medicine,
Kyoto University, Kyoto, Japan

Introduction

An ATP-driven efflux pump P-glycoprotein (Pgp), the multidrug resistance 1 (*MDR1* or *ABCB1*) gene product, is expressed in the plasma membrane of several tumor and normal cells and mediates extrusion of endogenous compounds, xenobiotics and drugs including anticancer drugs, cardiac glycosides, immunosuppressants, and anthracycline antibiotics (Ambudkar et al. 1999). Besides Pgp one of component molecules for the multidrug resistance of tumor cells, the transporter is now accepted as playing an important role for intestinal absorption, tissue distribution, and biliary or urinary excretion of drugs in normal tissues (Ambudkar et al. 1999).

Single nucleotide polymorphisms (SNPs) exist in the *MDR1* gene, and the relationship between SNPs and the expression/function of MDR1 has been reported by several laboratories. First, Hoffmeyer et al. (2000) represented that the C3435T SNP in the *MDR1* gene influenced the expression level of Pgp in the duodenum and that the absorption rate of orally administered digoxin was dependent on the SNP in healthy Caucasians. However, following examinations comparing SNPs in the *MDR1* gene with drug absorption and/or the intestinal expression level of Pgp, MDR1 have not been reproducible (Kim et al. 2001; Kurata et al. 2002; Goto et al. 2002; Gerloff et al. 2002). Recently, Siegsmund et al. (2002) demonstrated that the allele T of cDNA 3435 in the *MDR1* gene reduced Pgp expression in the kidney. However, there are few reports illustrating in detail the renal MDR1 expression with influences by its genetic variations.

Renal malignant tumors account for more than 2% of cancer incidence, and renal cell carcinoma (RCC) compose the majority in renal tumors. RCC shows resistance against chemotherapy (Hartmann and Bokemeyer 1999), and it is suggested that Pgp is involved in the chemoresistance of RCC (Fojo et al. 1987; Kakehi et al. 1988). Siegsmund et al. (2002) also suggested that

the C3435T SNP in the *MDR1* gene would be a risk factor for the development of RCC in Caucasians. In spite of suggesting the significance of Pgp and/or *MDR1* SNPs on the patients with RCC described above, the role of Pgp for chemoresistance of RCC has remained to be elucidated.

In the present study, we quantified the mRNA levels of MDR1 in the normal kidney cortex and RCC segments from Japanese nephrectomized patients with renal tumors. In addition, the ten common SNPs of the *MDR1* gene in these patients were examined, and the association between genotypes and expression level was assessed.

Materials and methods

Patients

Twenty-four Japanese patients who were surgically nephrectomized with RCC at Kyoto University Hospital were enrolled in this study. The subjects consisted of 18 men and six women whose ages ranged from 39 to 74 (63.6± 8.5, mean ± SD) years. The nephrectomized segments of the normal cortex and RCC were obtained after receiving written informed consent. The study was performed in accordance with the Declaration of Helsinki and its amendments, and was approved by the Ethics Committee of Kyoto University Graduate School and Faculty of Medicine.

Isolation of total RNA and genomic DNA

Total RNA and genomic DNA from a renal homogenate in a guanidinium thiocyanate solution were isolated with a MagNA Pure LC RNA isolation kit II and DNA isolation kit (Roche Diagnostic GmbH, Mannheim, Germany), respectively, as previously described (Goto et al. 2002; Motohashi et al. 2002). The isolated total RNA was reverse-transcribed, and the single stranded DNA was used for quantification of MDR1 mRNA levels. Genotyping of the *MDR1* gene was performed using genomic DNA.

Quantification of MDR1 mRNA expression levels

MDR1 mRNA levels in the normal kidney cortex and RCC segments were measured by real-time polymerase chain reaction (PCR), as previously described (Motohashi et al. 2002). The primer/probe set for the specific amplification of MDR1 was designed according to parameters incorporated in the Primer Express software (PE Biosystems, Foster City, CA, USA). The forward and reverse primers were GCTCAGACAGGATGTGAGTTGGT (position; 2812–2834, accession number M14758 in GenBank database) and CCTGGAACCTATAGCCCCTTTAAC (position; 2897–2920), respectively. The sequence of TaqMan probe was AAAAACACCACTGGAGCATTGACTACCAGG, corresponding to the position 2846-2875. Real-time PCR was performed in a total volume of 20 µl containing 2 µl of reverse-transcribed cDNA, 1 µM forward and reverse primers, 0.2 µM TaqMan probe, and 10 µl TaqMan Universal PCR Master Mix (Applied Biosystems, Foster City, CA, USA). The PCR condition was as follows: 50 cycles of 94°C for 15 s and 60°C for 60 s. The copy number of the target mRNA sequence in the starting materials was established by determining the fractional PCR threshold cycle number (Ct) at which a fluorescence signal generated during the replication process passed above a threshold value. The initial amount of target mRNA in each sample was estimated from the Ct value with a standard curve generated using known amounts of standard plasmid DNA. Glyceraldehyde-3-phosphate dehydrogenase mRNA was also quantified as an internal control with glyceraldehyde-3-phosphate dehydrogenase control reagent (Applied Biosystems).

Genotyping of the *MDR1* gene

The genotype of the *MDR1* gene was investigated by PCR-restriction enzyme fragment length polymorphism methods. The specific primers and restriction enzymes used in this study were as previously described (Goto et al. 2002). The PCR conditions were as follows: after denaturing at 94°C for 3 min, the PCR was performed with 1 µM of each primer and Taq DNA polymerase (Takara, Shiga, Japan), according to the following profile: 94°C for 30 s, 60°C for 30 s, and 72°C for 30 s, 35 cycles, following by a single additional 10-min extension at 72°C. The PCR products were digested with or without restriction enzymes and separated on 3.5% agarose gel.

Statistical analysis

The difference in the logarithmically transformed data of MDR1 mRNA expressions between normal cortex and RCC was analyzed using Student's paired *t*-test. The correlation between the *MDR1* genotype and its mRNA expression was analyzed using the Mann-Whitney *U* test. *P* values < 0.05 were considered to be significant.

Results

Quantification of MDR1 mRNA in normal kidney cortex and renal cell carcinoma

Figure 1 shows distribution histograms of logarithmically transformed mRNA levels of MDR1 in the normal kidney cortex and RCC segments. The average mRNA expression levels of MDR1 in the normal kidney cortex and RCC segments were 19.0 and 6.6 amol/µg total RNA, respectively. A statistical significant difference of the MDR1 mRNA levels in normal kidney cortex and RCC segments of each patient was observed ($P = 0.0042$, Fig. 2).

Genotype frequency of ten common SNPs of the *MDR1* gene in nephrectomized patients

The genotype of the *MDR1* gene from the normal kidney cortex and RCC segments was assessed at ten common nucleotide positions in 24 Japanese patients. No differences in *MDR1* genotypes from both segments of each patient were found. Frequencies of the genetic variants are summarized in Table 1. In this study, variants at exon 2–1, cDNA 61, cDNA 307, cDNA 1199, and exon 12 + 44 were not observed. A variant leading to amino acid exchange was observed only at cDNA 2677. The allele frequency of the cDNA 2677 was 45.8% for allele T and 18.8% for allele A. At cDNA 1236 and 3435, which do not influence amino acid substitute, genetic variants were recognized. Allele frequencies were 66.7% for allele T at cDNA 1236 and 52.1% for allele T at cDNA 3435. A complete linkage was observed

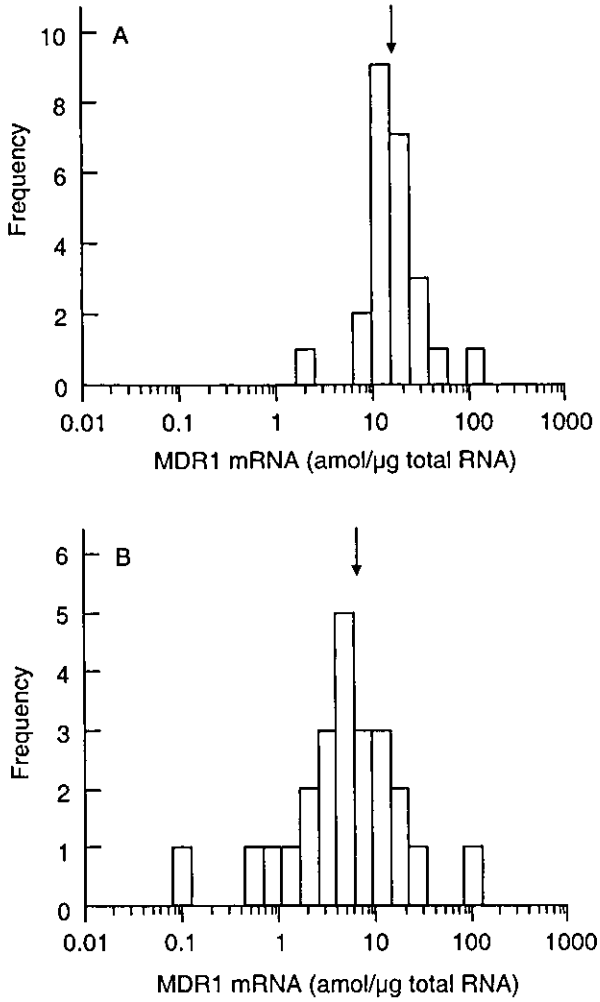

Fig. 1A, B Distribution histograms of MDR1 mRNA expression levels in normal kidney cortex (A) and renal cell carcinoma (B). MDR1 mRNA levels were logarithmically transformed to improve normality. The *arrows* indicate the mean values of MDR1 mRNA expression levels

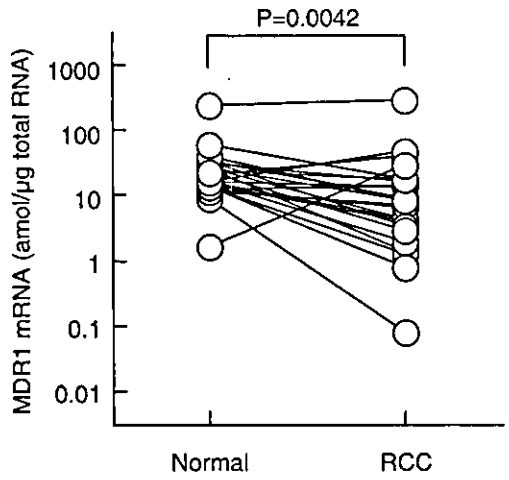

Fig. 2 Effect of malignant transformation on renal MDR1 mRNA levels in 24 patients with renal cell carcinoma

between cDNA 1236 C/T and an intronic variant of exon 6+139 C/T. Another intronic variant at exon 17–76 was determined with the frequency of 31.3% for allele A. These allele frequencies were comparable with our previous reports in Japanese recipients of living-donor liver transplantation.

Correlation between *MDR1* SNPs and MDR1 mRNA expression in normal kidney cortex and renal cell carcinoma

Next, we examined the association between the *MDR1* gene and its mRNA levels in the normal kidney cortex and RCC. As shown in Fig. 3, the significant effects of each SNP on MDR1 mRNA expression in the normal kidney cortex and RCC segments were not recognized. However, the MDR1 mRNA levels in the kidney were significantly reduced by transformation to RCC with C/T of cDNA 1236 and exon 6+139, T/A and T/T of exon 17–76, G/T of cDNA 2677, and C/T at cDNA 3435.

Discussion

In the present study, MDR1 mRNA levels in the human kidney cortex were quantified using the real-time PCR method. We previously examined its mRNA expression levels in the small intestine in Japanese recipients of living-donor liver transplantation. The MDR1 mRNA levels in the kidney cortex were about 40-fold higher than those in the intestinal mucosa (Goto et al. 2002; Hashida et al. 2001). Even if the mucosal samples derived from patients in end-stage liver failure were considered, the MDR1 mRNA contents in the kidney cortex were markedly higher compared to the intestine. To our knowledge, this is the first study of the quantification of MDR1 mRNA level in the human kidney cortex.

It is generally accepted that the majority of administered digoxin, a cardiac glycoside, is excreted into urine and that Pgp plays an important role for its tubular secretion (Tanigawara et al. 1992). In addition, concomitant administration with various drugs, including cyclosporin A, calcium channel blockers, macrolide antibiotics, and azole antifungal drugs elevates serum concentration of digoxin, at least in part, via renal tubular Pgp (Rodin and Johnson 1988; Wakasugi et al. 1998). Considering these pharmacokinetic significances of renal Pgp, the expression levels and activity of Pgp in the kidney would be a key factor for the optimal dosage regimen of digoxin.

The present findings represent a wide interindividual variation of MDR1 mRNA levels in the human kidney cortex (about 140-fold), and no relationship between the ten common SNPs of the *MDR1* gene and its mRNA expression levels. It was reported that the interindividual variation of MDR1 expression also existed in the human small intestine and liver, suggesting that expression variation has been responsible for interindividual